Patience is a Virtue: Optimal Investment in the Presence of Market Resilience

Nan Chen

Department of Systems Engineering and Engineering Management, The Chinese University of Hong Kong
nchen@se.cuhk.edu.hk

Min Dai

Department of Applied Mathematics, The Hong Kong Polytechnic University
mindai@polyu.edu.hk

Qiheng Ding and Chen Yang

Department of Systems Engineering and Engineering Management, The Chinese University of Hong Kong
qiheng@link.cuhk.edu.hk and cyang@se.cuhk.edu.hk

This paper investigates an optimal investment problem in an illiquid market, modeling explicitly the effects of three key features of market microstructure — market tightness, market depth, and finite market resilience — on the investor's decision. By employing a Bachelier process to model the dynamic of the fundamental value of the asset and assuming CARA-type utility for the investor, we manage to obtain the investor's optimal dynamic trading strategy in closed form by solving the resulting high-dimensional singular control problem. Furthermore, we extend the model to incorporate return-predicting signals and utilize an asymptotic expansion approach to derive approximate optimal trading strategies. The theoretical and numerical results emphasize the vital role of patience. Specifically, rather than dispersing small trades continuously over time as advocated by the existing literature, our findings suggest that investors should strategically time their trading activities to align with the aim portfolio in the presence of market resilience. To quantify this timing decision, we introduce a patience index that enables investors to strike a balance among various competing goals, including achieving currently optimal risk exposure, incorporating signals about future predictions, and minimizing trading costs, by leveraging market resilience.

Key words: Optimal investment; Market tightness; Market resilience; Singular control; Asymptotic expansion

1. Introduction

Optimal investment is of fundamental interest in financial economics. The classical paradigm, pioneered by Markowitz (1952), Sharpe (1964), and Merton (1969, 1971), emphasizes that investors must carefully balance between expected returns and risks when making investment choices. However, achieving such a balance in an optimal way becomes highly challenging in a dynamic market environment. On one hand, the literature documents well that expected returns of assets are predictable from various time-varying economic factors; see, e.g., Fama and French (1988), Ferson and Harvey (1993), Barberis (2000), and Koijen et al. (2009). To respond to changes in the return timely, active investors and fund managers need to build up accurate signals to predict security

returns and trade from their predictions for profits. Such practices necessitate frequent rebalancing of investment portfolios. On the other hand, markets can only provide limited liquidity at any given moment. Engaging in frequent and impatient trading incurs significant transaction costs, both directly from the bid-ask spread and indirectly from price impacts. Yet, the phenomenon of market resilience — the market's ability to replenish after trades — indicates that investors can avoid excessive trading costs if they can better utilize this dynamic aspect of market liquidity to defer trading appropriately into the future.

The benefit of patient trading is exemplified by the 2008 arbitrage crash in the US convertible bond market. The empirical study of Lewis et al. (2023) reveals that those convertible bond arbitrage hedge funds that were compelled to sell amid the looming market meltdown suffered from severe price discounts. In contrast, the traders who exercised patience or had alternative resources to postpone immediate selling mitigated effectively the risk of transacting at distressed fire-sale prices, as they could avoid the most unfavorable period of market liquidity. While this scenario represents an extreme case during a crisis, it underscores the importance of investors' choices between the current risk, expected return, immediate liquidity costs, and future transaction opportunities, in light of the evolution of market liquidity.

Motivated by the considerations outlined above, we investigate in this paper how the optimal trading strategies depend on the dynamics of market liquidity by proposing an optimal investment framework featuring both endogenously varying liquidity dynamics and return predictability. To the best of our knowledge, this is the first study to examine the interaction between these two crucial driving forces that underlie investors' decision-making. More precisely, (i) we take a stylized model to capture the three salient features of liquidity dynamics, as proposed by Kyle (1985): market tightness, finite market depth, and finite market resilience. In this model, trading activities widen the spread, leading to an inverse relationship between liquidity cost and market depth. Additionally, resilience gradually reduces costs over time as the market replenishes orders. As a result, the market liquidity is endogenous to the investor's trading activities. (ii) We assume that the investor constructs a signal process to predict asset returns and the predicting factor exhibits a mean-reverting pattern. Under this setup, the signal decays over time, reflecting the market reality that high expected returns are unlikely to persist for long once they emerge. Using mean-reverting processes to model the return predicting factor has been widely used in the optimal investment literature; see Kim and Omberg (1996), Campbell and Viceira (1999), Wachter (2002), Brokmann et al. (2023), Muhle-Karbe et al. (2023a), among others.

Our paper makes contributions from both the methodological and financial perspectives. Incorporating the above complex features of market liquidity and return predictability poses a methodological challenge because it leads to a singular control problem of high dimensionality. Nonetheless,

2

we successfully achieved a high level of tractability in this paper. Our approach tackles the problem in two steps. We first consider an optimal investment problem with constant returns as the base case. It corresponds to a 5-dimensional model. The presence of bid-ask spreads introduces to the optimal strategy a no-trade region, where the investor should refrain from trading unless their risky asset position deviates significantly from the optimal return-risk trade-off to avoid excessive transaction costs. Although these results share a similar structure as those in the traditional literature of proportional transaction costs (e.g., Shreve and Soner (1994), Liu (2004), Dai et al. (2009), and Chen et al. (2022)), the new feature of dynamic market resilience distinguishes our model significantly from these works. In particular, the bid-ask spread in our model changes over time due to the resilience, resulting in time-dependent trading boundaries for the no-trade region. We derive closed-form solutions to the optimal strategy in this case by reducing the determination of trading boundaries into solving a system of ordinary differential equations (ODEs). In contrast, the previous works can be regarded as investment problems under a constant bid-ask spread.

Building upon the insights gained from the base case solutions, we then propose as the second step an asymptotic expansion method to derive the approximate optimal strategy in closed form for the general case with a time-varying return-predicting signal. This problem presents an even greater challenge as it involves 6 dimensions. The approximate strategy obtained through this approach offers a high degree of interpretability, as shown below in the discussion on the financial contribution of our paper.

In terms of financial insights, our paper extends the general principle of "aim in front of target" proposed by Gârleanu and Pedersen (2013, 2016) to markets in which both tightness and resilience are present. In light of time-varying return-predicting signals and costly portfolio adjustments in illiquid markets, it is apparently suboptimal to invest myopically by trading all the way to the portfolio — referred to as the current Markowitz portfolio in their papers — that captures the best risk-return trade-off according to the current prediction. Their principle emphasizes that the optimal strategy, taking into account transaction costs, involves gradually incorporating the expected optimal Markowitz portfolio in the future toward which the current portfolio is moving, by smoothing out trading activities at a certain rate.

Note that market tightness, a crucial characteristic of market liquidity, is not explicitly modeled by Gârleanu and Pedersen (2013, 2016). However, incorporating this aspect yields fundamentally different implications compared to their works. Round-trip trades through buying and immediately selling are prohibitively costly if there exists a positive bid-ask spread[1]. Consequently, our model suggests that the investor should opt to halt trading, instead of dispersing small trades over time, when faced with adverse liquidity conditions in the market or weak predicting signals; leveraging

3

market resilience to replenish liquidity, the investor may exercise patience to await future trading opportunities.

Given the importance of trade timing as a crucial element of the optimal investment strategy when considering all three Kyle's illiquidity proxies, we develop a patience index from our explicit solutions to quantitatively determine the time to initiate trading activities. The index synergizes analytically the impacts of various factors that drive the investor's decision, including the market liquidity, investment time horizon, the investor's risk attitude, and the asset's riskiness. Consistent with our intuition, we find that, *ceteris paribus*, investors should exhibit greater patience in trading when they are in a less liquid market (particularly for our model, the market is shallower or less resilient), when dealing with a less risky asset, or when they are less risk averse.

As noted before, one advantage of working with the asymptotic expansion-based approach is that it offers financially interpretable strategies. Through it, we demonstrate how the investor uses the patience index to time trading to stay close to an aim portfolio, which is a weighted average of the current myopic portfolio and the optimal portfolio based on the long-run expected return, to achieve optimal investment performance. This is in line with the principle of "aim in front of target". However, the works of Gârleanu and Pedersen (2013, 2016) take a reduced form to model transaction costs. In comparison with their results, the weights in the construction of aim portfolios in our paper shed more insights on how the granular structure of the market liquidity, particularly the aforementioned three aspects of illiquidity, affect the investor's decision.

1.1. Literature Review

Besides the literature discussed above, our work is also related to the existing literature on optimal investment, return-predicting signals, and optimal execution.

1.1.1. Optimal investment in the presence of price impact.
There has been a large body of literature incorporating price impacts into the optimal investment model. The large body of the papers (e.g. Bank et al. (2017), Dai et al. (2023), Guasoni and Weber (2020, 2018), Muhle-Karbe et al. (2023a,b)) use the temporary (or instantaneous) price impact model, which assumes that while trading a large amount leads to extra cost due to the impact on the execution price, such impact will vanish instantly after the trading. However, existing empirical studies (e.g. Biais et al. (1995), Degryse et al. (2005), Kempf et al. (2009)) document the effect of market resilience and suggest that resilience is a market aspect independent of the spread. To study the effect of resilience, several papers use a reduced-form transient price impact model without the spread (e.g. Bank et al. (2015), Ekren and Muhle-Karbe (2019)).

Our base case model is closest to the transient price impact model that takes both the market resilience and the bid-ask spread into consideration (see Bank and Voß (2019), Roch and Soner

4

(2013), Soner and Vukelja (2016)). While Bank and Voß (2019) also study an optimal investment problem, their limit order book model differs from ours fundamentally, in that the best bid and ask prices revert to each other rather than to the fundamental price. Therefore, the resilience in their model is only embodied in the reduction of bid-ask spread but not in the reversion of midprice to fundamental price. In contrast, the resilience in our model is embodied in both. Furthermore, we allow for asymmetric market depth and resilience on bid and ask sides, while they assume symmetry. Our model for the limit order book is closer to the one considered in Soner and Vukelja (2016) (see also Roch and Soner (2013)), which focuses on the theoretical viscosity characterization. In contrast, we focus more on the analysis of the economic implication. Horst and Naujokat (2014) studied a stochastic target following problem under a similar limit order book setup. In addition to the base case model, we further study the general model to explore the interaction between market resilience and the return-predicting signal.

1.1.2. Return-predicting factors. Equity return predictability is widely acknowledged in literature; see Fama and French (1988), Ferson and Harvey (1993), Johannes et al. (2014), Koijen et al. (2009), and the references therein. In practice, there are many predictive signals on return used for trading. For example, at the higher frequency trading level, one can utilize indicators such as high-frequency trader demand (e.g. Brogaard et al. (2014)) or trader sentiment (e.g. Sun et al. (2016)) to predict the return over the next short period. At a lower frequency level, one can also utilize fundamental or macro economics factors to predict the return such as the dividend yield (e.g. Barberis (2000)).

The role of return-predicting factor in the optimal investment setting has been studied in literature; see Kim and Omberg (1996), Campbell and Viceira (1999), Wachter (2002), Gârleanu and Pedersen (2016), Brokmann et al. (2023), Muhle-Karbe et al. (2023a), among others. Different from these papers, our objective is to study the interaction between the return-predicting factor and the dynamic market liquidity and its impact on investors' patience.

1.1.3. Optimal execution. Our market liquidity model described in Section 3.1 is motivated by the models widely used in the optimal execution literature. In contrast to the optimal investment problem we consider, the optimal execution problem focuses on minimizing the trading cost in the process of achieving a target position (e.g. liquidating the starting stock position) within a given amount of time. Bertsimas and Lo (1998) and Almgren and Chriss (2001) study the optimal execution problem under both permanent and temporary price impact with the help of static exogenous price impact functions. Based on block-shaped limit order books, Obizhaeva and Wang (2013) studied an optimal execution problem with endogenous and dynamic liquidity featuring transient price impact. Later papers generalized this work to include general limit order book

5

shapes (Alfonsi et al. (2008)), multiple risky assets (Tsoukalas et al. (2019)), and asset return predictability (Haugh and Wang (2014)).

The rest of this paper is organized as follows. In Section 2, we present a dynamic model of market liquidity based on the celebrated setup used in Obizhaeva and Wang (2013) and a corresponding utility maximization problem. In Section 3, we develop optimal investment strategies in the base case with constant returns and the general case with return predictability. Section 4 contains numerical illustrations of our main theoretical results. Section 5 concludes the paper. All technical proofs are deferred to E-Companion.

2. Model Setup

In this section, we present an optimal investment model that incorporates the three important aspects of market liquidity as noted in the Introduction. Specifically, we describe a simple model for the dynamic market liquidity in Section 2.1. Based on this model, we formulate the investor's optimal investment problem in Section 2.2.

2.1. A Simple Model of Market Liquidity

Consider an investor equipped with a utility function $U(\cdot) : \mathbb{R} \to \mathbb{R}$ which is strictly concave, increasing, and bounded from above. Assume that the planning horizon is given by $[0, T]$. There are two types of assets available in the market, riskless cash and one risky "stock". Initially endowed with X_{0-} shares of stock and Y_{0-} dollars of cash, the investor has the objective of maximizing the expected utility over the wealth at T by trading these two assets. Assume that the fundamental price S_t of the stock follows the stochastic process

$$\mathrm{d}S_t = \mu \mathrm{d}t + \sigma \mathrm{d}W_t, \quad t \geq 0, \tag{1}$$

where μ and σ are both constants, representing the expected return and volatility, respectively, and $\{W_t, t \geq 0\}$ is a standard Brownian motion. In Section 3.2, we turn to investigate how the investor should respond to a time-varying return-predicting factor, characterized as a stochastic process μ_t in place of the constant μ in (1), in an illiquid market.

The primary interest of the paper is to characterize the impacts of three important aspects of the market liquidity — tightness, depth, and resilience — on the investor's trading decision. For ease of exposition, we follow Obizhaeva and Wang (2013) to assume that the stock trading is operated in a market organized through a limit order book (LOB) as shown in Figure 1. The advantage of working with this LOB based model is that it provides us with a parsimonious way to capture the aforementioned three aspects of market liquidity; refer to, e.g., Parlour and Seppi (2008) and Gould et al. (2013) for surveys on the economic and statistical issues of LOBs and the literature reviewed in Section 1.1 for other applications of similar LOB models.

6
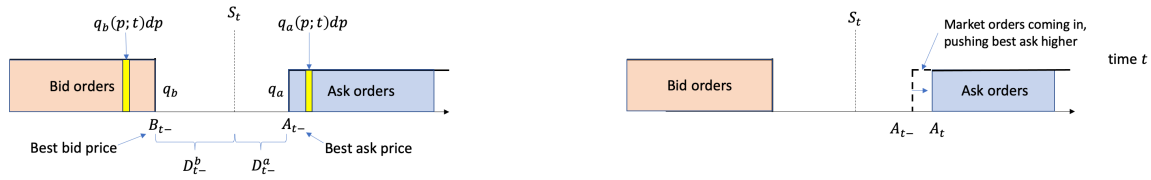
(a) The structure of LOB right before a chuck of buy market orders hits the market at time t.

(b) At time t, a market buy order enters the market. It is immediately executed and the execution pushes the best ask price from D_{t-}^a up to D_t^a.
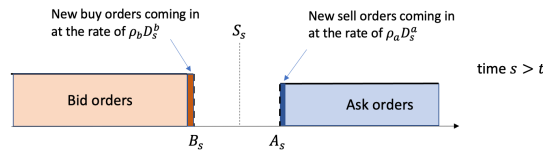
(c) At time $s > t$, an amount $\rho_b D_s^b ds$ of new buy orders come into the bid side of the book at the best bid price B_s within this moment. Meanwhile, an amount $\rho_a D_s^a ds$ of new sell orders are submitted at the best ask price A_s on the ask side of the LOB.

Figure 1   The block-shaped limit order book model

The market participants trade with each other based on two basic types of orders: limit orders and market orders. Limit orders specify the worst-case (or limit) price that traders intend to commit with to buy or sell a certain amount of the asset. One submitted buy (resp. sell) limit order will be executed if its limit price is higher (resp. lower) than the lowest (resp. highest) price of the sell (resp. buy) orders perching on the opposite side of the LOB. All unfulfilled orders will be recorded in the LOB as the available inventory in the market. In contrast, market buy (resp. sell) orders are immediately executed against the existing supply or demand in LOB at the current best ask (resp. bid) prices. Since we are interested in the price impacts generated by the investor, we assume that she only uses market orders to trade.

Panel (a) in Figure 1 displays three basic components of the LOB. First, the fundamental price S_t sits in between the unfulfilled buy and sell orders. Second, the two blocks of limit bid and ask orders provide liquidity to the market. The densities of limit orders in both blocks are given by two functions $q_a(p;t)$ and $q_b(p;t)$, respectively. In other words, $q_a(p;t)\mathrm{d}p$ (resp. $q_b(p;t)\mathrm{d}p$) shares of sell (resp. buy) limit orders are placed in the price interval $[p, p+\mathrm{d}p)$ for any \$$p$ higher (resp. lower) than the best ask (resp. bid) price at time t, waiting for being lifted off by the market orders in the future. For tractability, we assume $q_a(p;t)$ (resp. $q_b(p;t)$) to be time-invariant and characterized by

7

two step functions. More accurately, we have

$$q_a(p;t) = \begin{cases} 0, & p < A_t; \\ q_a, & p \geq A_t, \end{cases} \quad \left(\text{resp.} \quad q_b(p;t) = \begin{cases} 0, & p > B_t; \\ q_b, & p \leq B_t, \end{cases} \right) \tag{2}$$

for two constants q_a and q_b, where A_t and B_t are the respective best ask and bid prices at time t. Third, let D_t^a and D_t^b be the deviations of the current ask price A_t and bid price B_t from the fundamental price S_t, respectively; that is,

$$D_t^a = A_t - S_t \text{ (resp.} \quad D_t^b = S_t - B_t).$$

We hereafter refer to them as the ask (resp. bid) spread. The sum of $D_t^a + D_t^b$ constitutes the bid-ask spread at time t, reflecting the current *tightness* of the market, i.e., the cost of an immediate round-trip trade.

The block-shaped LOB densities in (2) imply linear price impacts. To illustrate this, let us consider the case of buy market orders. If a buy market order of size x ($x > 0$) is submitted at time t, the trade will be executed against the pending orders on the ask side of LOB. Denote D_{t-}^a and A_{t-} to be the ask spread and best ask price prior to the trade. Then, all the limit orders between the prices $A_{t-} = S_t + D_{t-}^a$ and $A_t = S_t + D_t^a$ will be lifted off by this market order, where the post-trade ask spread D_t^a satisfies

$$\int_{S_t+D_{t-}^a}^{S_t+D_t^a} q_a \mathrm{d}p = x; \tag{3}$$

see Panel (b) of Figure 1 for an illustration. Equation (3) shows that a market buy order of size x pushes D_{t-}^a up to

$$D_t^a = D_{t-}^a + \frac{x}{q_a}. \tag{4}$$

In this process, the total execution cost for this trade amounts to

$$\int_{S_t+D_{t-}^a}^{S_t+D_t^a} p q_a \mathrm{d}p = (S_t + D_{t-}^a)x + \frac{x^2}{2q_a} = A_{t-}x + \frac{x^2}{2q_a}. \tag{5}$$

According to (5), the trader has to pay additionally $x^2/(2q_a)$ on top of the best price A_{t-} observed right prior to the moment of order submission. Similarly, a sell market order of size x ($x < 0$) submitted at time t results in the total sale proceeds of

$$B_{t-}x - \frac{x^2}{2q_b}, \tag{6}$$

which is $x^2/(2q_b)$ less than the proceeds if the entire order could be sold at the best bid price B_{t-}.

Dividing both (5) and (6) by the transaction size $|x|$, we can see that the average additional buying (resp. selling) cost for each transacted share equals $|x|/(2q_a)$ (resp. $|x|/(2q_b)$). This impact

8

increases linearly with respect to the trade size $|x|$, but decreases with the limit order density q_a (resp. q_b). In this sense, we may regard q_a (resp. q_b) as the measure of the *market depth*, the second aspect of market liquidity, on the ask (resp. bid) side of this LOB. The literature has accumulated adequate empirical evidence that this kind of impact in the real market should be concave in the trading sizes; see, e.g., Bouchaud et al. (2009). As a special case of concave impact functions, the linear form is resulted in by the block-shaped assumption that we use to maintain the model tractability. In addition, this model allows the slopes of the linear impacts to be different across the bid and ask blocks. A study in Blais and Protter (2010) shows that such asymmetric linear functions fit the supply curve of less liquid stocks well.

The third component of this model is its *finite resilience*. After a trade, the enlarged ask (resp. bid) spread begets investors to submit new sell (resp. buy) orders at a lower (resp. higher) price. Thus, the liquidity consumed by the previous trades will be replenished. In practice, such replenishment is accomplished gradually. See, for instance, Biais et al. (1995), Hamao and Hasbrouck (1995), Degryse et al. (2005), Large (2007), and Lo and Hall (2015) for the empirical studies on market resilience.

To capture this dynamic aspect of market liquidity, we assume that the limit sell and buy orders in our model are replenished at the rates of $\rho_a > 0$ and $\rho_b > 0$, respectively. That means the ask (resp. bid) spread gets improved during the period of $[t, t + dt)$ by

$$dD_t^a = -\rho_a D_t^a \mathrm{d}t \quad (\text{resp. } dD_t^b = -\rho_b D_t^b \mathrm{d}t) \tag{7}$$

in the absence of trading at time t; see Panel (c) of Figure 1. Under (7), the larger the current ask/bid spread, the more aggressively liquidity providers step in to post new orders to offer liquidity at better prices. Combining (4) and (7), we can see that the liquidity dynamic in this market is endogenous to the investor's trading activities. In our setup, both the best bid price B_t and ask price A_t (and hence the mid price) revert to the fundamental price. This is in stark contrast to that of Bank and Voß (2019) where B_t and A_t revert to each other and the mid price does not necessarily revert to the fundamental price.

2.2. Trading Activities and Optimal Investment Problem

Let the nondecreasing processes L_t and M_t track the cumulative amounts of purchase and sale of the stock by the investor up to time t, respectively. Hence, the instantaneous increments $\mathrm{d}L_t$ and $\mathrm{d}M_t$ indicate the buy and sell amounts at time t, respectively, which are up to the decision of the investor. Under the trading strategy $\{(\mathrm{d}L_t, \mathrm{d}M_t), t \in [0, T]\}$, the stock holding of the trader at a given moment t will change according to the dynamic

$$\mathrm{d}X_t = \mathrm{d}L_t - \mathrm{d}M_t. \tag{8}$$

9

Remark 2.1 *Mathematically, we have more accurate descriptions on* $\mathrm{d}L_t$ *and* $\mathrm{d}M_t$. *By the celebrated Lebesgue decomposition of increasing functions (see, e.g., Chapter 3 in Stein and Shakarchi (2009)), the process* L_t *admits the following representation:*

$$L_t = L_t^c + \sum_{0 \le s \le t} \Delta L_s = \int_0^t l_s ds + \xi_t^L + \sum_{0 \le s \le t} \Delta L_s.$$

Here L_t^c *is continuous in* t *and* $\sum_{0 \le s \le t} \Delta L_s$ *is the pure jump part of process* L_t *with countably many jumps* $\Delta L_s = L_s - L_{s-} > 0$. *Furthermore,* L_t^c *consists of two components. The first one* $\int_0^t l_s ds$ *is absolutely continuous with respect to the Lebesgue measure, where* $l_s ds$ *is the number of shares to be purchased during the time interval* $[s, s + ds)$. *The second one* ξ^L *is singular with respect to the Lebesgue measure. We can show that the optimal strategy in our base case in Section 3.1 involves only the absolutely continuous parts (and the jump parts* ΔL_t *and* ΔM_t*), representing smooth trading at a finite speed. The singular part emerges in Section 3.2 when we incorporate trading signals, which involves the local time type trading at the boundaries of the no-trade region.*

Correspondingly, there are two parts of costs associated with the above trading strategy. If the trading occurs continuously according to the schedule $\mathrm{d}L_t^c$, then such trading can be fulfilled by the limit orders sitting on the best ask price, leading to a transaction cost of $A_t \mathrm{d}L_t^c$. On the other hand, if the investor chooses to submit a discrete trade of size ΔL_t at time t, that will incur a cost amounting to

$$\left(S_t + D_{t-}^a + \frac{\Delta L_t}{2q_a} \right) \Delta L_t = A_{t-}\Delta L_t + \frac{1}{2q_a}(\Delta L_t)^2$$

as implied by (5). A similar analysis applies for the selling strategy $\mathrm{d}M_t$. Assume the trader is self-financed and transacts on the basis of her cash account. In addition, for simplicity, assume that the risk free interest rate is zero. Putting everything together, we know that the value change in the balance of the trader's cash account in the infinitesimal interval $[t, t + \mathrm{d}t)$ is given by

$$\mathrm{d}Y_t = \underbrace{-A_t\mathrm{d}L_t^c - \left[A_{t-}\Delta L_t + \frac{1}{2q_a}(\Delta L_t)^2 \right]}_{\text{proceeds associated with stock purchase}} + \underbrace{B_t\mathrm{d}M_t^c + \left[B_{t-}\Delta M_t - \frac{1}{2q_b}(\Delta M_t)^2 \right]}_{\text{proceeds associated with stock sale}}. \tag{9}$$

As noted in Section 2.1, trading with market orders will impact the evolution of the ask and bid spreads D_t^a and D_t^b. In the presence of both the price impact (cf. (4)) and the market resilience (cf. (7)), we know that D_t^a (resp. D_t^b) evolves according to

$$\mathrm{d}D_t^a = -\rho_a D_{t-}^a \mathrm{d}t + \frac{1}{q_a}\mathrm{d}L_t \quad \left(\text{resp. } \mathrm{d}D_t^b = -\rho_b D_{t-}^b \mathrm{d}t + \frac{1}{q_b}\mathrm{d}M_t \right). \tag{10}$$

10

At time T, the terminal wealth owned by the trader is $S_T X_T + Y_T$, where we assume that the trader's stock holding is evaluated at the fundamental price S_T in the end. The trader needs to solve the following optimization problem:

$$\max_{\mathrm{d}L_t, \mathrm{d}M_t : t \in [0,T]} \mathbb{E}\left[U(S_T X_T + Y_T) | S_{0-}, X_{0-}, Y_{0-}, D_{0-}^a, D_{0-}^b\right] \tag{11}$$

subject to the state dynamics (1), (8), (9), and (10), where the expectation is calculated at time 0 conditional on $S_{0-} = s$, $X_{0-} = x$, $Y_{0-} = y$, $D_{0-}^a = d_a$, and $D_{0-}^b = d_b$.

3. Main Results

As noted in the Introduction, incorporating liquidity impacts into the investor's trading decision leads to challenging high dimensional control problems. We manage to obtain explicit solutions. This section presents the main results of the paper. Specifically, Section 3.1 analyzes a tractable base case in which the stock return remains constant over time. Using this result as a benchmark and the starting point, we proceed in Section 3.2 to investigate how to trade on the return signal in the presence of limited liquidity through an asymptotic expansion method. A patience index, which encodes the impacts of various market illiquidity factors on the investor's trading timing, is highlighted in Section 3.1.1.

3.1. Base Case with Exponential Utility

Having detailed the LOB model and the related optimal investment problem in Section 2, we now turn to derive its solution along with the optimal policies. To this end, define

$$V(t,s,x,y,d_a,d_b) = \max_{\mathrm{d}L_u, \mathrm{d}M_u : u \in [t,T]} \mathbb{E}\left[U(S_T X_T + Y_T) | S_{t-} = s, X_{t-} = x, Y_{t-} = y, D_{t-}^a = d_a, D_{t-}^b = d_b\right].$$

In other words, V presents the value function to the problem of (11) but with a sub-time horizon $[t, T]$. Using the Dynamic Programming Principle, we can show that V satisfies the following variational inequality: for any $t < T$,

$$\max\left\{ \underbrace{\mathcal{L}V}_{\text{No-trade}}, \quad \underbrace{\frac{1}{q_a}\frac{\partial V}{\partial d_a} + \frac{\partial V}{\partial x} - (s+d_a)\frac{\partial V}{\partial y}}_{\text{Buy}}, \quad \underbrace{\frac{1}{q_b}\frac{\partial V}{\partial d_b} - \frac{\partial V}{\partial x} + (s-d_b)\frac{\partial V}{\partial y}}_{\text{Sell}} \right\} = 0, \tag{12}$$

subject to the terminal condition $V(T,s,x,y,d_a,d_b) = U(xs + y)$, where the differential operator $\mathcal{L}$ is defined as

$$\mathcal{L}V = \frac{\partial V}{\partial t} + \mu\frac{\partial V}{\partial s} + \frac{1}{2}\sigma^2\frac{\partial^2 V}{\partial s^2} - \rho_a d_a\frac{\partial V}{\partial d_a} - \rho_b d_b\frac{\partial V}{\partial d_b}. \tag{13}$$

We defer the proof of (12) to E-Companion EC.1. However, the intuition of this variational inequality is clear. Consider any given time $t < T$. Assume that the fundamental price is $S_t = s$,

11

and the best ask and bid prices are $S_t + D_{t-}^a = s + d_a$ and $S_t - D_{t-}^b = s - d_b$, respectively. The investor has three options at this moment. As the first option, she can choose to buy the stock. If she decides to buy δx (an infinitesimal amount) shares, she needs to pay at the best ask price for this purchase out from her cash holdings. That will result in a value change for V amounting to

$$\underbrace{\delta x \cdot \frac{\partial V}{\partial x}}_{\substack{\text{value change caused} \\ \text{by stock position}}} - \underbrace{(s+d_a)\delta x \cdot \frac{\partial V}{\partial y}}_{\substack{\text{value change caused} \\ \text{by cash position}}}.$$

In addition, as noted in (4), the trade impacts D_t^a as well, changing it to $d_a + \delta x / q_a$. Hence, the value change in V caused by this price impact will be

$$\frac{\delta x}{q_a} \cdot \frac{\partial V}{\partial d_a}$$

In total, the decision of purchasing δx shares of the stock will lead to an aggregate effect on V by

$$\delta x \cdot \left(\frac{1}{q_a} \frac{\partial V}{\partial d_a} + \frac{\partial V}{\partial x} - (s+d_a)\frac{\partial V}{\partial y} \right).$$

The second option is that the investor can choose to sell δx shares of the stock. Following a similar derivation as above, we know that this sale will generate a value change of V given by

$$\delta x \cdot \left(\frac{1}{q_b} \frac{\partial V}{\partial d_b} - \frac{\partial V}{\partial x} + (s-d_b)\frac{\partial V}{\partial y} \right).$$

The third option available for the trader is to remain inactive in the trading during $[t, t+\mathrm{d}t)$. Recall that three market variables, S_t, D_t^a, and D_t^b evolve according to (1) and (7). The term of $\mathcal{L}V$ captures the expected changes in V due to the evolution of these variables. In particular, the first three terms in (13) represent the marginal effect of the change in the fundamental price of S on V, while the last two terms summarize the expected changes in V due to the changes of D_t^a and D_t^b, respectively. The trader maximizes her utility over the aforementioned three options. That is why we have the variational inequality characterized in (12).

The problem contains one temporal and five state variables. We find that it is tractable under some specific setups, particularly if the investor is equipped with a CARA utility. Suppose that the investor's preference is prescribed by $U(x) = 1 - \exp(-\gamma x)$ with the constant absolute risk aversion parameter $\gamma > 0$. In a frictionless market (i.e., when the market depth $q_a, q_b \to +\infty$, the resilience $\rho_a, \rho_b \to +\infty$, and the bid and ask spreads $d_a = d_b = 0$ in our model), it is well-known in the literature (see, e.g. Bank and Voß (2019)) that the following buy-and-hold strategy is optimal:

$$\mathrm{d}L_t^{NF} = \left(\frac{\mu}{\sigma^2 \gamma} - X_t \right)^+ \quad \text{and} \quad \mathrm{d}M_t^{NF} = \left(X_t - \frac{\mu}{\sigma^2 \gamma} \right)^+.$$

12

In words, absent any market frictions, the trader should immediately buy (or sell) the discrepancy, if any, between $\mu/(\sigma^2\gamma)$ and the asset holding that she has at time t. Note that $\mu/(\sigma^2\gamma)$ is the solution to the celebrated Merton's investment problem for a trader with the exponential utility; see Merton (1969, 1971). It captures the impact of the asset fundamentals on the trader's investment by striking optimally the balance between the asset excess return μ and its riskiness σ. We will refer to $\mu/(\sigma^2\gamma)$ as the *Merton portfolio* hereafter.

However, such a myopic strategy is too aggressive in the presence of limited liquidity because it may cause excessive impact costs. As we are about to show, there exists a subregion in the state space under the optimal strategy of the problem (11) such that the trader should remain inactive whenever the conditions of the subregion are met. Let $\mathcal{S}$ denote the state space of the problem:

$$\mathcal{S} = \{(x, d_a, d_b) : x \in \mathbb{R}, \ d_a \geq 0, \ d_b \geq 0\} \subset \mathbb{R}^3.$$

Under the assumption of CARA utility, we can show that the investor's optimal strategy does not depend on the stock fundamental value s and the cash position y. That is why a 3-dim state space is adequate. Let $h_a(t)$ and $h_b(t)$ be two increasing and strictly positive functions defined in (EC.8), which do not depend on state variables. We have

Theorem 3.1 *For any given time $t \in [0, T)$, the state space $\mathcal{S}$ can be divided into three subregions as follows:*

$$\text{Buy region:} \qquad \mathcal{BR}_t = \left\{(x, d_a, d_b) \in \mathcal{S} : x - \frac{\mu}{\sigma^2\gamma} \leq -h_a(t)d_a\right\}, \qquad (14)$$

$$\text{Sell region:} \qquad \mathcal{SR}_t = \left\{(x, d_a, d_b) \in \mathcal{S} : x - \frac{\mu}{\sigma^2\gamma} \geq h_b(t)d_b\right\}, \qquad (15)$$

$$\text{No-trade region:} \qquad \mathcal{NR}_t = \mathcal{S}\backslash(\mathcal{BR}_t \cup \mathcal{SR}_t). \qquad (16)$$

We can define an optimal strategy $\{(\mathrm{d}L_t^*, \mathrm{d}M_t^*) : t \in [0, T]\}$ to solve the original problem (11).

Note that $\mathcal{BR}_t \cap \mathcal{SR}_t = \emptyset$. Correspondingly, the boundaries of both trading regions are given by

$$\partial\mathcal{BR}_t = \left\{(x, d_a, d_b) \in \mathcal{S} : x - \frac{\mu}{\sigma^2\gamma} = -h_a(t)d_a\right\}$$

and

$$\partial\mathcal{SR}_t = \left\{(x, d_a, d_b) \in \mathcal{S} : x - \frac{\mu}{\sigma^2\gamma} = h_b(t)d_b\right\},$$

respectively. Figure 2 displays the above three subregions in the $(d_a|d_b, x - \mu/(\sigma^2\gamma))$-plane for a given t. Here, we use $d_a|d_b$ to denote a system of double horizontal axes. In other words, starting from the origin, the horizontal d_b-axis points to the right and the d_a-axis to the left. The vertical
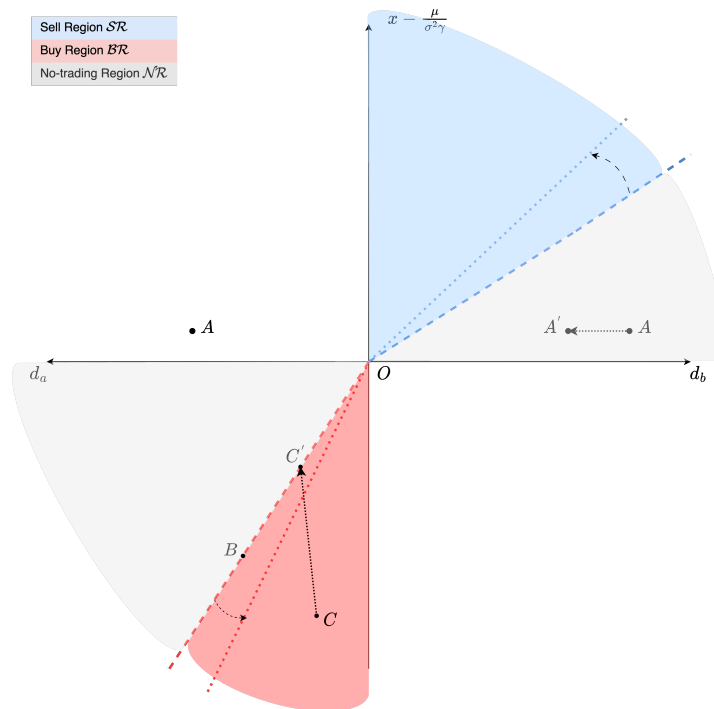
13

Figure 2 **The trading and no-trade regions. We use a plane in the figure to represent the state space $\mathcal{S}$. The vertical axis shows $X - \mu/(\sigma^2\gamma)$, the difference between the current position and the Merton portfolio. The right and left parts of the horizon axis represent d_b and d_a, respectively. The blue and red shaded regions correspond to the sell region ($\mathcal{SR}$) and buy region ($\mathcal{BR}$), respectively. The sell/buy boundaries will rotate in the direction of arrows over time.**

axis shows the excess amount of the stock holding over the Merton portfolio at t. Any $(x, d_a, d_b) \in \mathcal{S}$ can then be represented by a pair of points in such a plane. For instance, the pair of two points, denoted by A in both the first and second quadrant of the plane in Figure 2, represents an investor whose stock position at time t is slightly larger than the Merton portfolio (i.e., positive $x - \mu/(\sigma^2\gamma)$) in a market with the corresponding d_A and d_B as the bid and ask spreads.

By the expression of boundary $\partial \mathcal{SR}_t$, we can use a straight line in the first quadrant of the above $(d_a|d_b, x - \mu/(\sigma^2\gamma))$-plane to depict it. The slope of this straight line is given by $h_b(t)$. The sell region $\mathcal{SR}_t$ at time t corresponds to the part above the sell boundary $\partial \mathcal{SR}_t$; refer to the blue region and the corresponding dashed line in Figure 2 for illustration. The gray region underneath the sell boundary in the first quadrant corresponds to one part of the no-trade region $\mathcal{NR}_t$. Symmetrically, we have the red shaded region and the bordering dashed line in the third quadrant of Figure 2 to represent the buy region $\mathcal{BR}_t$ and its boundary $\partial \mathcal{BR}_t$, respectively. The slope of $\partial \mathcal{BR}_t$ is determined by $h_a(t)$. The gray region above the red buy region in the third quadrant constitutes the other part of $\mathcal{NR}_t$.

14

With the help of the three subregions, we can explicitly specify the optimal trading strategy for the investor. Define, at each time $t \in [0, T]$, the following feedback policy (dL_t^*, dM_t^*) prescribing to each state $(x, d_a, d_b) \in \mathcal{S}$ the action the investor needs to take. We establish the optimality of the above strategy rigorously in EC.2.

- **Inactive**: if $(x, d_a, d_b) \in \mathcal{NR}_t$, $dL_t^* = dM_t^* = 0$. Point A in Figure 2 exemplifies this case. The investor currently owns more stocks than the Merton portfolio. However, she also faces a relative high bid spread d_b, i.e.,

$$\frac{x - \mu/(\sigma^2 \gamma)}{h_b(t)} < d_b.$$

As a result, she should wait for trading opportunities in the future. Point A horizontally moves towards the vertical axis (e.g. in the direction of A') as both d_b and d_a revert to 0 over time.

- **Gradual buying**: if $(x, d_a, d_b) \in \partial\mathcal{BR}_t$, $dL_t^* = l_t^* dt$ and $dM_t^* = 0$ with the rate of purchase given by

$$l_t^* = \frac{\rho_a h_a(t) - h_a'(t)}{h_a(t)(1 + h_a(t)/q_a)} \left(\frac{\mu}{\sigma^2 \gamma} - x \right). \tag{17}$$

Point B in Figure 2 stands for this case. According to (10), this gradual buying activity will generate impacts on the ask spread, leading its change rate in $[t, t + dt]$ to be

$$\left(-\rho_a D_t^a + \frac{l_t^*}{q_a} \right) dt.$$

- **Lump-sum buying**: if $(x, d_a, d_b) \in \mathcal{BR}_t \backslash \partial\mathcal{BR}_t$, i.e., the state is in the interior of the buy region (see Point C in Figure 2 for example). In this case, the number of shares x of the trader is far less than the benchmark Merton portfolio. Thus the trader should immediately place a lump-sum purchase order $dL_t^* = \Delta L_t^*$ with

$$\Delta L_t^* = \frac{1}{1 + h_a(t)/q_a} \left(\frac{\mu}{\sigma^2 \gamma} - x \right) - \frac{h_a(t) d_a}{1 + h_a(t)/q_a}. \tag{18}$$

This trading activity generates instantaneously two folds of impacts. First, it reduces the distance of the trader's stock holding to the Merton portfolio. Second, it enlarges the ask spread from d_a to $d_a + \Delta L^*/q_a$. We can show that the new location of the trader's portfolio immediately after this purchase in the $(d_a|d_b, x - \mu/(\sigma^2 \gamma))$-plane must be on the boundary $\partial\mathcal{BR}_t$. In Figure 2, we use Point C' to illustrate the two impacts. Note that the horizontal coordinate of C' is larger than that of C, indicating the price impact caused by this trade in terms of the ask spread d_a. Meanwhile, the absolute value of $x - \mu/(\sigma^2 \gamma)$ of Point C' is lower than that of C because the trade partially corrects the excess part of the current stock holding compared with the Merton portfolio.

15

- **Gradual selling**: if $(x, d_a, d_b) \in \partial\mathcal{SR}_t$, $\mathrm{d}L_t^* = 0$ and $\mathrm{d}M_t^* = m_t^*\mathrm{d}t$ with the rate of sale given by

$$m_t^* = \frac{\rho_b h_b(t) - h_b'(t)}{h_b(t)(1 + h_b(t)/q_b)}\left(x - \frac{\mu}{\sigma^2\gamma}\right).$$

- **Lump-sum selling**: if $(x, d_a, d_b) \in \mathcal{SR}_t \setminus \partial\mathcal{SR}_t$, $\mathrm{d}L_t^* = 0$ and $\mathrm{d}M_t^* = \Delta M_t^*$ with the lump-sum sale amount equal to

$$\Delta M_t^* = \frac{1}{1 + h_b(t)/q_b}\left(x - \frac{\mu}{\sigma^2\gamma}\right) - \frac{h_b(t)d_b}{1 + h_b(t)/q_b}. \tag{19}$$

3.1.1. Patience Index As illustrated in (14)-(16), the investor under the optimal policy should tolerate deviations in her stock holdings from the Merton portfolio to some extents because of the liquidity concern. Namely, given the state (X_t, D_t^a, D_t^b), she will not start trading unless

$$-h_a(t)D_t^a < X_t - \frac{\mu}{\sigma^2\gamma} < h_b(t)D_t^b \tag{20}$$

is breached. In this sense, we refer to $h_b(t)D_t^b$ and $-h_a(t)D_t^a$ as *indices of the patience to buy and to sell* for the investor, respectively. As the first implication, these indices suggest that investors should be more patient when the current bid or ask spread is large: higher D_t^a or D_t^b, more difficult the inequality (20) will be violated when the investor starts from the no-trade region. This prediction is consistent with the empirical findings in the futures market (see Wang and Yau (2000)) and options market (see George and Longstaff (1993)) that the trading volume is negatively correlated to the bid-ask spread.

Further investigating these two indices, we can see that there are two opposing considerations at play in determining the investor's timing choice. Figure 2 can help us better understand the underlying intuition. On one hand, the market resilience leads to a decrease in both d_a and d_b. The expectation of declining transaction costs over time will incentivize the investor to defer trades into the future. For instance, consider Point A in Figure 2. It is initially in the no-trade region at time t. As time goes by, d_a decreases, causing A to move horizontally in the direction of A' towards the trading boundary $\partial\mathcal{SR}$. On the other hand, since this is a finite-horizon problem, the benefits of deferring trading relative to the associated impact costs diminish as time approaches T. This effect, referred to as the time effect later, is captured by the monotonically increasing nature of both $h_b(t)$ and $h_a(t)$ with respect to t. When t increases, both boundaries $\partial\mathcal{SR}$ and $\partial\mathcal{BR}$ will rotate counterclockwise, resulting in dwindled trading regions (as depicted by the movement from dashed lines to dotted lines in Figure 2).

Calculating the time derivatives of both patience indices casts more insights on how they characterize the interplay of the aforementioned two opposing effects. Taking the patience to sell as an example, if there is no trade at t,

$$\frac{\mathrm{d}}{\mathrm{d}t}(h_b(t)D_t^b) = \left(\frac{h_b'(t)}{h_b(t)} - \rho_b\right)h_b(t)D_t^b. \tag{21}$$
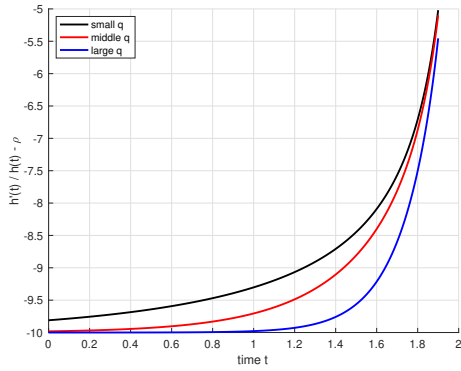
16

Note that ρ_b is the rate of reversion in the bid spread, reflecting how fast the transaction cost will be reduced because of the market resilience. In contrast, the term $h_b'(t)/h_b(t)$ characterizes the rotation rate of boundary $\partial \mathcal{SR}$. According to (21), the relative strength of the two quantities determines the change of the patience to buy over time.
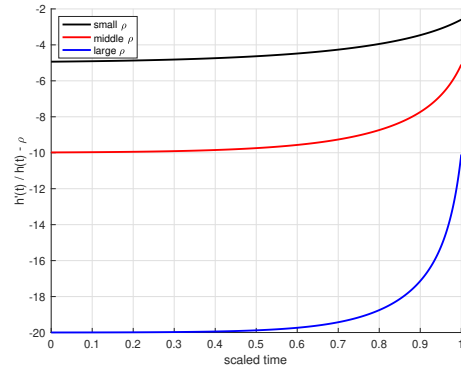
In general, we have, for $i = a, b$,

$$
\mathrm{sgn}\left(\frac{\mathrm{d}}{\mathrm{d}t}(h_i(t)D_t^i) \right) = \begin{cases} -1 & \text{if } t \in \left[0, T - \frac{1}{\rho_i}\right); \\[2mm] +1 & \text{if } t \in \left[T - \frac{1}{\rho_i}, T\right], \end{cases} \tag{22}
$$

where $\mathrm{sgn}(\cdot)$ is the *signum* function that returns the sign of a real number. Eq. (22) yields two implications. First, when the remaining trading horizon is long, namely, when $T - t > 1/\rho_i$, the patience $h_i(t)D_t^i$ decreases over time according to the negative sign of its derivative. In this case, the market resilience is a dominant factor relative to the time effect captured by $h_i'(t)/h_i(t)$. If the trader posits in the no-trade region now because of a high bid or ask spread, then she will choose to wait until the moment that the resilience brings $h_i(t)D_t^i$ down to a level equal to $x - \mu/(\gamma\sigma^2)$ to start trading. Second, when $T - t \leq 1/\rho_i$, the positive derivative of $h_i(t)D_t^i$ implies that the patience increases over time in this case. This is because the impacts caused by trading outweigh the benefit of portfolio rebalancing for a short investment horizon. As a result, when the trader starts with a portfolio in the no-trade region at $t \in [T - \frac{1}{\rho_i}, T]$, she will not trade at all in the remaining time horizon.
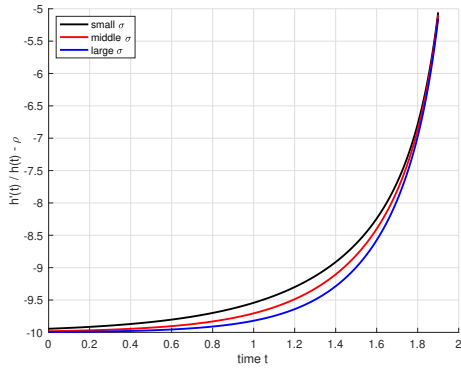
Figure 3 shows the comparative statics of the derivative of log-patience $\frac{\mathrm{d}}{\mathrm{d}t}\log(h_i(t)D_t^i)$ with respect to the other liquidity related parameters, the investor's risk aversion coefficient, and the stock's riskiness in a long remaining time horizon. Figure 3 (a) and (b) exhibit the comparative statics with respect to the market depth q and resilience rates ρ_a or ρ_b, respectively. For larger q or ρ, i.e., more liquid markets, the derivative $\frac{\mathrm{d}}{\mathrm{d}t}\log(h_i(t)D_t^i)$, $i = a, b$, will have larger absolute values. Since $\log(\cdot)$ is a monotone function, this implies that the patience indices decay faster over time in a more liquid market. By (20), the investor will be less patient in the sense that she will start to trade earlier when she start from the no-trade region. Figure 3(c) and (d) show the effects of the volatility σ of the stock's fundamental price and the investor's risk-aversion coefficient γ on $\frac{\mathrm{d}}{\mathrm{d}t}\log(h_i(t)D_t^i)$, $i = a, b$. The more risk averse for the investor or the riskier the stock, the faster the values of $h(t)D_t$ reduces over time. This indicates that the investor will trade more impatiently when dealing with either a more risky stock or she is more risk averse.
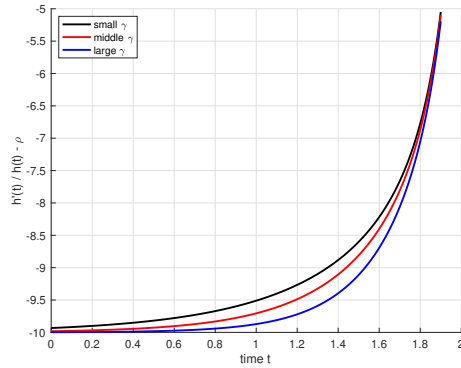
17

(a) different q

(b) different ρ

(c) different σ

(d) different γ

Figure 3 Function $\frac{h'(t)}{h(t)} - \rho$ for $t \in [0, T - 1/\rho)$. From (21), this function determines the decaying rate of the patient indices. The default parameters used in the figure are $\rho = 10$, $q = 10$, $\sigma = 0.2$, $\gamma = 1$, and $T = 2$. In (a), we draw the function graph under $q = 2, 10, 50$, keeping everything else identical as the default values; in (b), $\rho = 5, 10, 20$; in (c), $\sigma = 0.15, 0.2, 0.25$; in (d), $\gamma = 0.5, 1, 2$. We omit the subscript $i = a, b$ for h, ρ, q. In plot (b), note that different ρ leads to different time horizon $[0, T - 1/\rho)$. We plot the function graph using a scaled time horizon $t/(T - 1/\rho)$ to make sure that we can compare function values within the same range.

3.2. The Role of Predictive Return Signals

In the above analysis we have assumed a constant expected return μ for the fundamental price. In the following, we study the impact of stochastic return-predicting signals on the optimal strategy. Specifically, we extend the fundamental price model from (1) to

$$\mathrm{d}S_t = \mu_t \mathrm{d}t + \sigma \mathrm{d}W_t, \quad t \geq 0,$$

with μ_t given by the Vasicek model

$$\mathrm{d}\mu_t = \kappa(\bar{\mu} - \mu_t)\mathrm{d}t + \beta \mathrm{d}W'_t. \tag{23}$$

Here, $\bar{\mu}$ is the long-run mean return, κ is the speed at which μ_t reverts to $\bar{\mu}$, β is the volatility of the signal, and $\{W', t \geq 0\}$ is another standard Brownian motion independent of W following the

18

setup of Gârleanu and Pedersen (2016). Note that incorporating predictive signals will add one more dimension compared to the model in Section 3.1. We do not expect exact solutions in explicit form in this case. To maintain numerical tractability, we apply an asymptotic expansion approach to solve the resulting singular control problem.

To this end, introduce a scaling parameter $\varepsilon \geq 0$ to (23) by letting

$$d\mu_t^\varepsilon = \varepsilon\left[\kappa(\bar\mu - \mu_t^\varepsilon)dt + \beta dW_t'\right].$$

We may interpret ε as the "strength" of the signal. In particular, when $\varepsilon = 1$, we restore the original process (23) and taking $\varepsilon = 0$ leads to the constant expected return case as discussed in Section 3.1. Define the corresponding value function that the investor can obtain starting from time t by

$$V^\varepsilon(t, s, \mu, x, y, d_a, d_b)$$
$$= \max_{dL_u, dM_u: u \in [t,T]} \mathbb{E}\left[U(S_T X_T + Y_T)|S_{t-} = s, X_{t-} = x, Y_{t-} = y, D_{t-}^a = d_a, D_{t-}^b = d_b, \mu_{t-}^\varepsilon = \mu\right]. \quad (24)$$

Following the derivation leading to (12), we know that V^ε satisfies the following variational inequality

$$\max\left\{\mathcal{L}^\varepsilon V^\varepsilon, \quad \frac{1}{q_a}\frac{\partial V^\varepsilon}{\partial d_a} + \frac{\partial V^\varepsilon}{\partial x} - (s + d_a)\frac{\partial V^\varepsilon}{\partial y}, \quad \frac{1}{q_b}\frac{\partial V^\varepsilon}{\partial d_b} - \frac{\partial V^\varepsilon}{\partial x} + (s - d_b)\frac{\partial V^\varepsilon}{\partial y}\right\} = 0. \quad (25)$$

The equation (25) shares a similar structure as (12) with the three terms on the left hand side corresponding to no-trading, buying, and selling, respectively. The only difference between (25) and (12) lies in the differential operator $\mathcal{L}^\varepsilon$ representing no-trading. It is now given by

$$\mathcal{L}^\varepsilon V = \frac{\partial V}{\partial t} + \mu\frac{\partial V}{\partial s} + \frac{1}{2}\sigma^2\frac{\partial^2 V}{\partial s^2} + \varepsilon\kappa(\bar\mu - \mu)\frac{\partial V}{\partial \mu} + \frac{1}{2}\varepsilon^2\beta^2\frac{\partial^2 V}{\partial \mu^2} - \rho_a d_a\frac{\partial V}{\partial d_a} - \rho_b d_b\frac{\partial V}{\partial d_b}.$$

$\mathcal{L}^\varepsilon V$ contains two additional terms involving the first and second derivatives of V with respective to the new state variable μ, reflecting the impact of signal changes on the optimal value.

When ε is sufficiently small, we can asymptotically expand the value function to derive explicit expressions for the optimal regions. This approach yields high interpretability as the resulting explicit solutions provide valuable economic insights on how signals and market liquidity consideration jointly affect the investor's strategies. Cai et al. (2018) applies a similar methodology to a different context of capital gains taxes. See also Chen et al. (2022) for another application of the asymptotic expansion approach in correlated assets with proportional transaction costs.

The approach consists of two steps. First, we posit the following Ansatz for V^ε:

$$V^\varepsilon(t, s, \mu, x, y, d_a, d_b) = 1 - \exp\{-\gamma[y + sx + F^\varepsilon(t, \mu, x, d_a, d_b)]\}.$$

19

Substituting it back to (25), we can see that F^ε satisfies

$$\max\left\{\mathcal{L}_F^\varepsilon F^\varepsilon, \quad \frac{1}{q_a}\frac{\partial F^\varepsilon}{\partial d_a} + \frac{\partial F^\varepsilon}{\partial x} - d_a, \quad \frac{1}{q_b}\frac{\partial F^\varepsilon}{\partial d_b} - \frac{\partial F^\varepsilon}{\partial x} - d_b\right\} = 0, \tag{26}$$

with

$$\mathcal{L}_F^\varepsilon F = \frac{\partial F}{\partial t} + \mu x - \frac{1}{2}\sigma^2\gamma x^2 + \varepsilon\kappa(\bar\mu - \mu)\frac{\partial F}{\partial \mu} + \frac{1}{2}\varepsilon^2\beta^2\left[\frac{\partial^2 F}{\partial \mu^2} - \gamma\left(\frac{\partial F}{\partial \mu}\right)^2\right] - \rho_a d_a\frac{\partial F}{\partial d_a} - \rho_b d_b\frac{\partial F}{\partial d_b}$$

and $F^\varepsilon(T, \mu, x, d_a, d_b) = 0$. Through this Anzatz and (26), we reduce the dimensionality of problem (25) down to 5. As the second step, we further expand F^ε in terms of ε to

$$F^\varepsilon(t, \mu, x, d_a, d_b) = F_0(t, \mu, x, d_a, d_b) + \varepsilon F_1(t, \mu, x, d_a, d_b) + O(\varepsilon^2). \tag{27}$$

Using (27), together with the corresponding expansions on the boundaries of sell and buy regions (refer to (EC.17)), we can decompose the variational inequality (26) into two iterative PDEs of F_0 and F_1 (refer to (EC.18)–(EC.19)). Based on the above approach, we prove in E-Companion EC.4:

Theorem 3.2 (Asymptotic Trading Regions with Return Signal) *For a given ε, denote*

$$\hat\mu_t^i = (1 - \varepsilon r_i(t))\mu_t + \varepsilon r_i(t)\bar\mu, \quad i = a, b. \tag{28}$$

We have the following approximations to the optimal regions:

$$\text{Buy region:} \qquad \widehat{\mathcal{BR}}_t^\varepsilon = \left\{(x, d_a, d_b) \in \mathcal{S} : x - \frac{\hat\mu_t^a}{\sigma^2\gamma} \leq -h_a(t)d_a\right\},$$

$$\text{Sell region:} \qquad \widehat{\mathcal{SR}}_t^\varepsilon = \left\{(x, d_a, d_b) \in \mathcal{S} : x - \frac{\hat\mu_t^b}{\sigma^2\gamma} \geq h_b(t)d_b\right\},$$

$$\text{No-trade region:} \qquad \widehat{\mathcal{NR}}_t^\varepsilon = \mathcal{S}\backslash(\widehat{\mathcal{BR}}_t^\varepsilon \cup \widehat{\mathcal{SR}}_t^\varepsilon).$$

Here, $h_a(t)$ and $h_b(t)$ are defined as in Theorem 3.1, and $r_a(t)$ and $r_b(t)$ are defined in (EC.20). These functions only depend on time and model parameters, but not state variables.

The regions in Theorem 3.2 resemble those in the base case (cf. (14), (15), and (16)), up to the first order terms of ε. The investor will not start buying (resp. selling) unless

$$X_t > \frac{\hat\mu_t^a}{\sigma^2\gamma} - h_a(t)D_t^a \quad \left(\text{resp. } X_t < \frac{\hat\mu_t^b}{\sigma^2\gamma} + h_b(t)D_t^b\right) \tag{29}$$

is breached at some time t. In other words, the investor aims at two benchmark portfolios $\hat\mu_t^a/(\gamma\sigma^2)$ (resp. $\hat\mu_t^b/(\gamma\sigma^2)$) and she will start to transact if her stock holdings are excessively low (resp. high) compared with them.

According to (28),

$$\frac{\hat\mu_t^i}{\gamma\sigma^2} = (1 - \varepsilon r_i(t))\frac{\mu_t}{\gamma\sigma^2} + \varepsilon r_i(t)\frac{\bar\mu}{\gamma\sigma^2}, \quad i = a, b. \tag{30}$$

A salient feature of the construction of the above aim portfolios is that they are in fact a weighted average between the Merton portfolio based on the current return-predicting signal μ_t, and the expected Merton portfolio in the long run. Since μ_t changes over time, the Merton portfolio $\mu_t/(\gamma\sigma^2)$ is now a moving target. Thus, trading all the way to tracing such a target is not optimal in the presence of market illiquidity. Theorem 3.2 implies that the investor should maintain her portfolio close to such aim portfolios to both partly capture the best current risk-return trade off and incorporate the dynamic effect of μ_t.

The weight $\varepsilon r_i(t)$ balancing the current and expected future portfolios in the construction (30) is computable via (EC.20). Figure 4 displays its comparative statics with respect to a variety of parameters including investment time horizon t, market depth q, market resilience ρ, and the mean-reverting speed κ of the predicting signal. When t approaches T, $r_i(t)$ decreases to 0, indicating

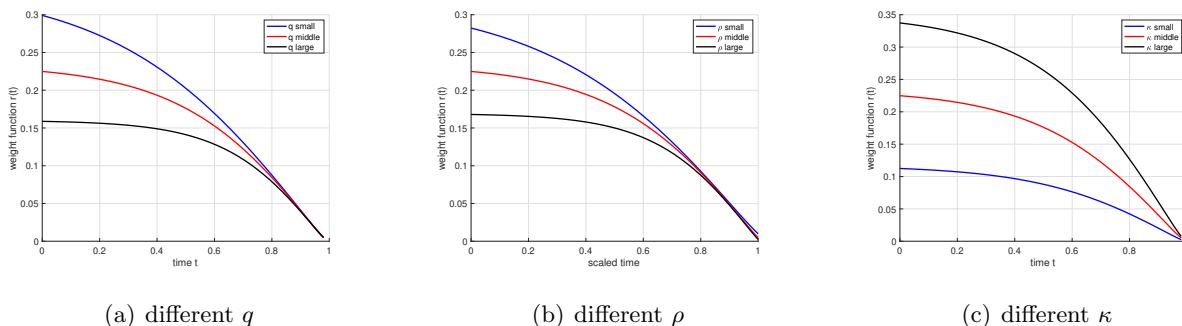| (a) different q | (b) different ρ | (c) different κ |

Figure 4 **Weight function $r(t)$ with respect to time t. The default parameters used in the figure are $\sigma = 0.25$, $\gamma = 1$, $\rho = 50$, $q = 10$, $T = 1$, $\bar{\mu} = 0.1$, $\kappa = 1$, and $\beta = 0.1$. For (a), we take $q = 5, 10, 20$ and keep the other parameters identical to the default values; for (b), $\rho = 25, 50, 100$; for (c), $\kappa = 0.5, 1.0, 1.5$. We omit the subscript $i = a, b$ for h, ρ, q. In plot (b), note that different ρ leads to different time horizon $[0, T - 1/\rho]$. We plot the function graph using a scaled time horizon $t/(T - 1/\rho)$ to make sure that we can compare function values within the same range.**

that the investor will gradually shift her aim to the current Merton portfolio as time goes by. This is consistent with our intuition, since as the remaining horizon decreases, it is increasingly unlikely that μ_t will revert to the long-term average $\bar{\mu}$ by the terminal time T. As a result, the expected optimal portfolio in the long run becomes less relevant in the aim.

As the market becomes more illiquid, i.e., ρ or q decrease, Figure 4(a) and (b) show that $r_i(t)$ becomes larger. In other words, when the illiquidity is high, the investor should put more weight on tracking the long-term Merton portfolio, because closely following the current Merton portfolio requires frequent and costly portfolio rebalancing. Furthermore, the value of $r_i(t)$ is affected by the signal's persistence as well. This can be observed by altering the parameter κ in Figure 4(c), while keeping the other parameters constant. It is evident from this plot that a smaller κ leads a greater weight to the current Merton portfolio in the construction of the aim portfolio. Note that

21

μ_t exhibits slower changes when κ is smaller. This conveys an intuitive economic message that the investor should trade more aggressively on persistent signals than on fast mean-reverting signals: the current value μ_t lasts longer periods under a persistent signal and thus the investor can benefit more from aligning trades more with μ_t. Finally, the weight is also scaled by ε, the strength of the signal. The previous base case is just a special example of (30) when we take $\varepsilon = 0$.

The above findings are closely related to the general principles of "aim in front of target" and "trade gradually towards the aim" proposed in Gârleanu and Pedersen (2013, 2016) for the investors facing transaction costs. However, richer structures of market illiquidity in our model, particularly the market tightness captured by the bid-ask spreads, bring in new insights. Absent the bid-ask spreads, Gârleanu and Pedersen (2013, 2016) argue that the investor in their model should trade continuously according to a finite speed. In a stark contrast, our results underscore the importance of the *timing* of trading. Whenever the market variables are in $\widehat{\mathcal{NR}_t^{\bar{\varepsilon}}}$, it is optimal to defer trading and wait. The value of waiting in the general case lies in not only taking advantage of the market resilience for a smaller spread as suggested in the base case in Section 3.1, but also waiting for a suitable predictive return signal. The conditions in (29) explicitly capture this observation. Note that transactions can be triggered by both the changes in patience indices $h_b(t)D_t^b$ and $h_a(t)D_t^a$, which encode the influence of improved market liquidity on the investor's trading decision as explained in Section 3.1, and the changes in $\hat{\mu}_t^i$, which embodies the effect of signals.

Moreover, as an extension of Gârleanu and Pedersen (2013, 2016), our model accommodates imbalance markets in the sense that the market depths and resilience are different on the bid and ask sides; in other words, both sides are allowed to have different level of liquidity. Theorem 3.2 shows that the weights r_b and r_a should be different under asymmetric depth and resilience on the bid and ask sides, leading to two different aim portfolios to track when the investor considers sell and buy decisions.

We can derive approximate optimal trading strategies from the above state space decomposition in Theorem 3.2. Similar to Section 3.1, they consist of three types of trading activities: inactive, lump-sum buying or selling, and gradual buying or selling. Specifically, we encapsulate $(\mathrm{d}L_t^*, \mathrm{d}M_t^*)$, the resulting approximate optimal buying and selling amounts at time t, as follows:

- **Inactive**: if $(x, d_a, d_b) \in \widehat{\mathcal{NR}_t^{\bar{\varepsilon}}}$, $\mathrm{d}L_t^* = \mathrm{d}M_t^* = 0$.
- **Lump-sum buying and selling**: if (x, d_a, d_b) is in the interior of the buy region $\widehat{\mathcal{BR}_t^{\bar{\varepsilon}}}$, $\mathrm{d}M_t^* = 0$ and the investor should immediately place a lump-sum purchase order

$$\mathrm{d}L_t^* = \Delta L_t^* = \frac{1}{1 + h_a(t)/q_a} \left(\frac{\hat{\mu}_t^a}{\sigma^2 \gamma} - x \right) - \frac{h_a(t)d_a}{1 + h_a(t)/q_a}. \tag{31}$$

On the other hand, if (x, d_a, d_b) is in the interior of the sell region $\widehat{\mathcal{SR}_t^{\bar{\varepsilon}}}$, $\mathrm{d}L_t^* = 0$ and

$$\mathrm{d}M_t^* = \Delta M_t^* = \frac{1}{1 + h_b(t)/q_b} \left(x - \frac{\hat{\mu}_t^b}{\sigma^2 \gamma} \right) - \frac{h_b(t)d_b}{1 + h_b(t)/q_b}. \tag{32}$$

22

The strategy $(\mathrm{d}L_t^*, \mathrm{d}M_t^*)$ takes a feedback form by associating each state (x, d_a, d_b) with a particular action. Like (18) and (19), the investor uses the lump-sum selling and buying strategies in (31) and (32) to correct her current stock holding when she finds that it is excessively larger or smaller than the aim portfolios.

However, incorporating predictive signals into the model causes an additional technicality complication on the part of gradual buying and selling strategy. Just imagine the investor is in the no-trade region $\widehat{\mathcal{NR}_t^\varepsilon}$ now; refer to Point A in Figure 2. In addition to decreasing d_a or d_b coordinates, the movement of the point corresponding to the investor's state contains an additional vertical Brownian component because its $x - \mu_t/(\sigma^2\gamma)$ coordinate changes over time due to μ_t. When this point happens to be on the boundary $\partial\mathcal{SR}_t$ at time t, it will move "frequently" in and off the sell region driven by the Brownian part of μ_t. Thus a precise description of the investor's strategy at t should be based on the local time of a diffusion process as discussed in EC.5. We include the following simple definition to complete the presentation of $(\mathrm{d}L_t^*, \mathrm{d}M_t^*)$ and refer interested readers to EC.5 for more technical discussions.

- **Gradual buying and selling**. Let $\{k_t^i : t \geq 0\}$, $i = a, b$, be the local time processes associated with the diffusion process defined in EC.5. If (x, d_a, d_b) is on the boundary $\partial\widehat{\mathcal{BR}_t^\varepsilon}$, $\mathrm{d}L_t^* = dk_t^a$ and $\mathrm{d}M_t^* = 0$. Similarly, if $(x, d_a, d_b) \in \partial\widehat{\mathcal{SR}_t^\varepsilon}$, $\mathrm{d}L_t^* = 0$ and $\mathrm{d}M_t^* = -\mathrm{d}k_t^b$.

To further discern the connection and differences between the above policy and the principle of aiming in front of target advocated by Gârleanu and Pedersen (2013, 2016), we use Figure 5 to visually present a typical sample trajectory of the investor's stock holding positions over time in response to the evolution of signals when she follows our dynamic policy. To this end, we simulate one sample path of μ_t based on (23). Then we plot the corresponding target position $\mu_t/(\sigma^2\gamma)$ as the red solid line, which represents the optimal holding in a frictionless market. Meanwhile, we also plot the position changes under our optimal trading strategy (blue solid line) and the aim portfolios constructed from the weighted average $\hat{\mu}_t$ in (28) (black dashed line).

We see that the aim portfolios, which the investor attempts to track down, are forward-looking. When the current signal μ_t is higher than its long-term average $\bar{\mu}$ (see, for instance, the period around $t = 0.2$ in Figure 5), it is expected to fall in the future. Incorporating this future movement, the aim portfolio around $t = 0.2$ is smaller than the Merton portfolio $\mu_t/(\sigma^2\gamma)$ based on the current signal μ_t. On the other hand, the aim portfolio around $t = 0.4$ is larger than the current Merton portfolio at that time because the signal is anticipated to rise back to its long run average. Our dynamic trading strategy tends to keep close to the aim portfolios. As shown by Figure 5, it tends to buy as the aim portfolio increases and to sell otherwise. In this sense, our dynamic trading strategy aligns with the principle of aiming in front of target.
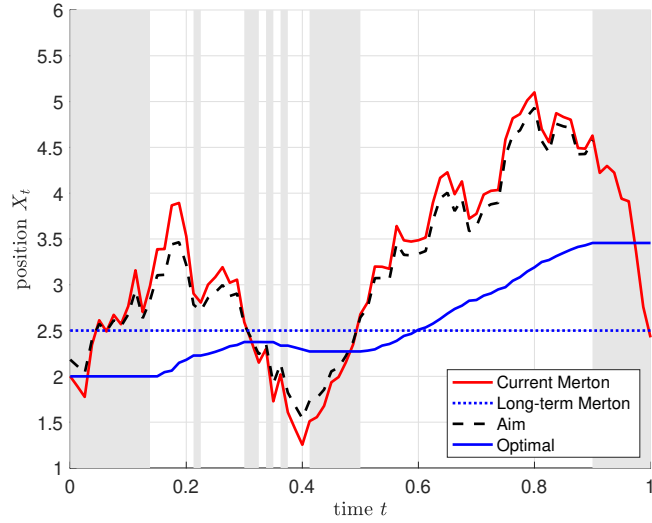
23

Figure 5 **The evolution of stock holding position** X_t **under the optimal trading strategy** $(\mathrm{d}L_t^*, \mathrm{d}M_t^*)$ **along a sample path of signal** μ_t. **The red solid line presents the current Merton portfolio** $\mu_t/(\sigma^2\gamma)$. **The blue dotted line shows the long-term Merton portfolio** $\bar{\mu}/(\sigma^2\gamma)$, **which does not change over time. Use the black dashed line and blue solid line to display the aim portfolio** $\hat{\mu}_t/(\sigma^2\gamma)$ **and investor's stock holding, respectively. The current Merton portfolio is generated from one simulated trajectory of** μ_t. **The gray areas correspond to the time periods in which the investor remains inactive, i.e.** X_t **remains constant over such periods. The default parameter values used in the figure are** $\gamma = 1$, $\rho = 10$, $q = 10$, $T = 1$, $\bar{\mu} = 0.1$, $\sigma = 0.2$, $\kappa = 1$, $\beta = 0.1$ $\varepsilon = 1$, $\mu_0 = 0.08$, $D_0^a = D_0^b = 0.05$, **and** $X_0 = 2$.

In consideration of the impacts of market liquidity, the portfolio adjustment under our dynamic trading strategy is much smoother compared to the updating in the signal. Represented by the gray zones in the figure, a salient feature of the simulated path of stock positions is that the investor will pause trading for a significant amount of time. Take the initial period in Figure 5 for example. The investor does not start to buy the stock until a late stage, although the signal increases quickly over time. This patience is mainly driven by the large spread we set for the experiment: the investor intends to wait for a stronger signal and a reduced spread to enter the market. In a sharp contrast, the trading strategy in the works of Gârleanu and Pedersen (2013, 2016) continuously adjusts investment portfolios.

4. Numerical Experiments

In this section, we present numerical experiments based on our model and discuss their economic implications. The default values for the model parameters are described as follows. The investment horizon T and the initial stock price S_{0-} are normalized to be 1 year and \$1, respectively. We use 252 days as the day-count convention for 1 year. The annualized volatility and long-run expected growth rate of the stock price are respectively given by $\sigma = 25\%$ and $\bar{\mu} = 0.1$, which correspond to a Sharpe ratio of 0.4. The risk aversion coefficient is $\gamma = 0.5$. Under these parameter values, the

24

long-term Merton portfolio for the investor is $\bar{\mu}/(\sigma^2\gamma) = 3.2$. We set the market depth $q_a = q_b = 32$, meaning that the investor will generate a 10% price impact if she purchases the long-run Merton portfolio immediately at time 0 starting from zero position. In addition, we take $\varepsilon = 1$ to examine the performance of our approximation approach on the original model.

As for the market resilience, we take $\rho_a = \rho_b = 126$ as the default values for both ask and bid sides. Under such choices, by (7), we have

$$D_{t+\frac{1.39}{252}}^i = D_t^i \exp\left(-\rho_i \times \frac{1.39}{252}\right) = 0.5 D_t^i, \quad i = a, b.$$

In words, the market takes 1.39 days to replenish orders to shrink the ask (resp. bid) spreads to half after being impacted by a buy (resp. sell) order. Following Obizhaeva and Wang (2013), we refer to 1.39 days as the corresponding half-life of such ρ. In the subsequent experiments, we also test a range of resilience values: $\rho \in \{4.1589, \ 8.3178, \ 16.6355, \ 33.2711\}$, which are corresponding to a half-life of 2 months, 1 month, 0.5 months, and 5.25 days.

Finally, for the signal process, we take its volatility $\beta = 20\%$ and the mean-reversion speed $\kappa = 1.3863$. From the marginal probability density of the Vasicek model (see, e.g., Shreve (2004), Section 4.4), we know that

$$\mathbb{E}[\mu_{t+s} - \bar{\mu}] = \exp(-\kappa s)(\mu_t - \bar{\mu}).$$

Since $\exp(-1.3863 \times 0.5) = 0.5$, we can see that the signal will decay to half of its original strength in 0.5 year. $\kappa \in \{8.3178, \ 4.1589, \ 0.6931, \ 0.2773\}$ are also used in the numerical experiments. These values correspond to the half-life of the signal ranging from 1 month, 2 months, 1 year, to 2.5 years. For the other initial state variables, we set $(X_{0-}, Y_{0-}, D_{0-}^a, D_{0-}^b, \mu_0) = (0, 1, 0.1, 0.1, 0.1)$.

The theoretical analysis in Section 3 highlights the importance of striking a delicate balance between market liquidity considerations and predicting signals to achieve optimal investment performance. We compare our approximate optimal strategy, denoted by *opt* hereafter, with the optimal strategy in the absence of price impacts in Section 4.1 and with two trading strategies that solely focus on market liquidity impacts while disregarding the dynamics of the predicting signal in Section 4.2, respectively. By conducting these comparisons, we aim to demonstrate the advantages of our approximate optimal strategy in the context of market liquidity and predicting signals.

4.1. Patient Trading vs. Impatient Trading

To show the benefit of patient trading, consider an "impatient" alternative strategy *mer* that trades constantly to maintain the current Merton portfolio $\mu_t/(\sigma^2\gamma)$ according to μ_t. This strategy is actually optimal in a market with infinite liquidity. We define the certainty equivalent of two strategies by

$$\mathbb{E}\left[U(S_T X_T^j + Y_T^j)\right] = U(CE^j), \quad j \in \{opt, \ mer\},$$

25

where (X_T^j, Y_T^j) represent respectively the stock and cash positions at T when the investor follows the strategy j. In other words, CE^j is the certain amount of wealth equivalent to the random wealth by following strategy j from an initial wealth of 1. We run a Monte Carlo simulation with 2 million sample trajectories of $\{\mu_t : t \in [0,T]\}$ and $\{S_t : t \in [0,T]\}$ and follow the state dynamics in Section 2 to evaluate the expectations in the above definition of CE.

Table 1   Certainty Equivalent Difference between Optimal Strategy and Merton Strategy

		CE^{opt}	ΔCE^{mer}	CE^{opt}	ΔCE^{mer}	CE^{opt}	ΔCE^{mer}
		$\mu_0 = 0.1$		$\mu_0 = 0.08$		$\mu_0 = 0.12$	
I	Default	1.234	17.087	1.208	16.948	1.262	17.238
			(0.000)		(0.000)		(0.000)
II	$\gamma = 0.25$	1.432	67.378	1.386	66.945	1.491	67.869
			(0.002)		(0.001)		(0.002)
	$\gamma = 1.00$	1.123	4.409	1.110	4.359	1.138	4.462
			(0.000)		(0.000)		(0.000)
III	$\kappa = 8.3178$	1.149	17.053	1.144	16.904	1.156	17.213
			(0.000)		(0.000)		(0.000)
	$\kappa = 4.1589$	1.175	17.073	1.163	16.926	1.185	17.232
			(0.000)		(0.000)		(0.000)
	$\kappa = 0.6931$	1.274	17.095	1.242	16.962	1.313	17.242
			(0.000)		(0.000)		(0.001)
	$\kappa = 0.2773$	1.314	17.106	1.276	16.977	1.360	17.246
			(0.001)		(0.001)		(0.000)
IV	$\rho = 4.1589$	1.076	282.402	1.067	282.124	1.086	283.640
			(0.111)		(0.189)		(0.231)
	$\rho = 8.3178$	1.124	197.190	1.109	196.749	1.140	197.658
			(0.032)		(0.018)		(0.024)
	$\rho = 16.6355$	1.163	112.512	1.144	112.229	1.183	112.795
			(0.004)		(0.004)		(0.004)
	$\rho = 33.2711$	1.190	59.929	1.170	59.734	1.216	60.138
			(0.001)		(0.001)		(0.001)
V	$\beta = 0.1000$	1.169	4.685	1.141	4.556	1.198	4.824
			(0.000)		(0.000)		(0.000)
	$\beta = 0.3000$	1.334	37.759	1.311	37.607	1.358	37.924
			(0.001)		(0.001)		(0.001)
VI	$\sigma = 0.2000$	1.335	41.368	1.296	41.079	1.377	41.685
			(0.001)		(0.001)		(0.001)
	$\sigma = 0.3000$	1.171	8.349	1.153	8.270	1.192	8.435
			(0.000)		(0.000)		(0.000)

Note: The certainty equivalents and the differences are calculated via a Monte Carlo estimator with two million sample trajectories for both S and μ, where there are 5000 time steps on each trajectory. The standard errors of the differences of certainty equivalents are reported in the parenthesis.

Table 1 reports the performance of two trading strategies as measured by their certainty equivalent under different parameter values. In it, the columns of ΔCE^{mer} display the difference $CE^{opt} -$

CE^{mer}, with the quantities in the parenthesis showing the standard errors of the difference estimates for reference. The table contains 6 parts. Subpart I reports the outcomes under the default values of the parameters described at the beginning of this section, and Subparts II–VI focus on the comparative statics when we vary the investor's risk aversion coefficient, the mean-reversion speed of signal, the market resilience, the signal's volatility, and the stock fundamental volatility. All the results of ΔCE^{mer} are positive with statistical significance, indicating that our dynamic strategy outperforms strategy mer by a considerable margin for a large range of parameter values. In particular, one can see that the dominance of opt in terms of ΔCE^{mer} is most significant when the resilience ρ is small or the signal volatility β is large. As noted in Section 1, strategy mer necessitates frequent rebalancing of the investor's portfolio, especially if the signal is very volatile. Thus it will incur enormous trading costs when the market is illiquid (e.g., small ρ). Our dynamic strategy overcomes this shortcoming by trading patiently to strike better balance between market liquidity and return signal.

Table 2   **Trading Volume and Market Liquidity**

	Volume		
	$\mu_0 = 0.1$	$\mu_0 = 0.08$	$\mu_0 = 0.12$
Default	15.791	15.391	16.199
$\rho = 4.1589$	5.218	4.984	5.459
$\rho = 8.3178$	7.241	7.006	7.480
$\rho = 16.6355$	9.169	8.918	9.427
$\rho = 33.2711$	11.278	10.986	11.577
$q = 4$	8.311	8.042	8.582
$q = 8$	10.245	9.929	10.562
$q = 16$	12.722	12.366	13.089

Note: The trading volumes are calculated via a Monte Carlo estimator with two million sample trajectories for both S and μ, where there are 5000 time steps on each trajectory.

Table 2 examines the impacts of market liquidity, particularly resilience ρ and market depth q, on the trading volume under our dynamic trading strategy. Similar as Table 1, we divide $T = 1$ year into 5,000 time steps and simulate 2 million sample trajectories of S and μ using Monte Carlo. Calculate (L_t^*, M_t^*) along each pair of sample trajectory of (S_t, μ_t). The trading volume for each sample is then defined by

$$\sum_{n=1}^{5000} \{|L_{t_n}^* - L_{t_{n-1}}^*| + |M_{t_n}^* - M_{t_{n-1}}^*|\},$$

where $\{t_n : n = 1, \cdots, 5000\}$ are the discretized time steps. Table 2 displays the average volumes under different ρ and q. Obviously, the trading volumes increase as either ρ or q increases. This

indicates that the investor should be more active in trading for a more liquid market. These observations generate the following testable implications:

TESTABLE HYPOTHESIS I: Trading volumes are positively correlated with the market resilience

TESTABLE HYPOTHESIS II: Trading volumes are positively correlated with the market depth. We leave empirical studies on the relationship between market resilience/depth and trading activeness for future work.

4.2. The Economic Significance of Signal

In Section 4.1, we have illustrated the impacts of incorporating liquidity consideration on the optimal strategy. Now, we demonstrate the effects of signal in guiding efficient investments, by comparing our strategy *opt* against two alternative strategies — referred to as *myo* and *long* below — that do not fully utilize the dynamics of the predictive return signal. To this end, we use the same idea presented in Theorem 3.2 to construct the no-trade, buy, and sell regions for defining *myo* (myopic) and *long* (long-sighted). The only difference lies in that we replace the aim portfolio (28) in our dynamic trading strategy with $\mu_t/(\gamma\sigma^2)$ to define *myo* or $\bar{\mu}/(\gamma\sigma^2)$ to define *long*, respectively. Apparently, while these alternative strategies takes into account the liquidity impacts, they do not consider the evolution of signals.

As in Table 1, we estimate via Monte Carlo simulation the differences between the certainty equivalent of CE^{opt} and these two alternative strategies CE^{myo} and CE^{long}. Denote $\Delta CE^{myo} = CE^{opt} - CE^{myo}$ and $\Delta CE^{long} = CE^{opt} - CE^{long}$. Table 3 reports such comparison under various parameters. It shows that our optimal strategy consistently outperforms the two alternative strategies in all cases, as evidenced by its higher certainty equivalent.

The table reveals three additional patterns worth mentioning. Firstly, the advantage of our strategy over the *long*, as measured by ΔCE^{long}, becomes more pronounced as κ decreases. This is because the signal process exhibits greater persistence for smaller κ values, making it more crucial to track the Merton portfolio based on the current signal in order to achieve optimal investment performance. The aim portfolio constructed as from (28) contains a component of $\mu_t/(\gamma\sigma^2)$ while the *long* strategy completely disregards such information.

In contrast, ΔCE^{myo} exhibits an inverted U shape in relation to κ. In other words, the out-performance of strategy *opt* over the *myo* strategy is maximized for intermediate levels of κ. This pattern can be explained as follows. The aim portfolio under *opt* is constructed based on $\hat{\mu}$. For very small κ, it assigns more weights on the current Merton portfolio; see Figure 4(c). As a result, the difference between *opt* and *myo* diminishes. Conversely, when κ is very large, the signal process quickly reverts back to its long-term mean, and therefore μ_t will remain close to $\bar{\mu}$ over time. In this scenario, the aim portfolio tracked by our trading strategy closely aligns with $\mu_t/(\gamma\sigma^2)$, which is followed by *myo*.

28

Table 3 Certainty Equivalent Difference between Optimal Strategy and Alternative Strategies

		CE^{opt}	ΔCE^{long}	ΔCE^{myo}	CE^{opt}	ΔCE^{long}	ΔCE^{myo}	CE^{opt}	ΔCE^{long}	ΔCE^{myo}
			$\mu_0 = 0.1$			$\mu_0 = 0.08$			$\mu_0 = 0.12$	
I	Default	1.234	0.101	0.006	1.208	0.108	0.005	1.262	0.098	0.008
			(0.001)	(0.000)		(0.000)	(0.000)		(0.000)	(0.000)
II	$\gamma = 0.25$	1.432	0.177	0.023	1.386	0.192	0.017	1.491	0.169	0.029
			(0.001)	(0.000)		(0.001)	(0.000)		(0.001)	(0.000)
	$\gamma = 1.00$	1.123	0.056	0.002	1.110	0.059	0.001	1.138	0.055	0.002
			(0.000)	(0.000)		(0.000)	(0.000)		(0.000)	(0.000)
III	$\kappa = 8.3178$	1.149	0.005	0.011	1.144	0.005	0.007	1.156	0.005	0.014
			(0.000)	(0.000)		(0.000)	(0.000)		(0.000)	(0.000)
	$\kappa = 4.1589$	1.175	0.033	0.013	1.163	0.034	0.011	1.185	0.031	0.017
			(0.000)	(0.000)		(0.000)	(0.000)		(0.000)	(0.000)
	$\kappa = 0.6931$	1.274	0.150	0.003	1.242	0.161	0.002	1.313	0.145	0.005
			(0.001)	(0.000)		(0.001)	(0.000)		(0.001)	(0.000)
	$\kappa = 0.2773$	1.314	0.195	0.001	1.276	0.211	0.001	1.360	0.189	0.002
			(0.001)	(0.000)		(0.001)	(0.000)		(0.001)	(0.000)
IV	$\rho = 4.1589$	1.076	0.038	0.042	1.067	0.042	0.036	1.086	0.035	0.049
			(0.000)	(0.000)		(0.001)	(0.000)		(0.001)	(0.000)
	$\rho = 8.3178$	1.124	0.054	0.038	1.109	0.061	0.032	1.140	0.050	0.044
			(0.001)	(0.000)		(0.000)	(0.000)		(0.000)	(0.000)
	$\rho = 16.6355$	1.163	0.068	0.029	1.144	0.075	0.024	1.183	0.062	0.035
			(0.000)	(0.000)		(0.000)	(0.000)		(0.000)	(0.000)
	$\rho = 33.2711$	1.190	0.078	0.019	1.170	0.087	0.015	1.216	0.074	0.023
			(0.000)	(0.000)		(0.001)	(0.000)		(0.000)	(0.000)
V	$\beta = 0.10$	1.169	0.026	0.002	1.141	0.031	0.001	1.198	0.024	0.003
			(0.000)	(0.000)		(0.000)	(0.000)		(0.000)	(0.000)
	$\beta = 0.30$	1.334	0.219	0.014	1.311	0.228	0.012	1.358	0.212	0.017
			(0.001)	(0.000)		(0.001)	(0.000)		(0.001)	(0.000)
VI	$\sigma = 0.20$	1.335	0.144	0.014	1.296	0.156	0.010	1.377	0.135	0.018
			(0.000)	(0.000)		(0.001)	(0.000)		(0.001)	(0.000)
	$\sigma = 0.30$	1.171	0.075	0.003	1.153	0.080	0.002	1.192	0.074	0.004
			(0.000)	(0.000)		(0.000)	(0.000)		(0.001)	(0.000)

Note: This table shares a similar structure as Table 1. The certainty equivalents and the differences are calculated via a Monte Carlo estimator with two million sample trajectories for both S and μ, where there are 5000 time steps on each trajectory. The standard errors of the differences of certainty equivalents are reported in the parenthesis.

Secondly, as we increase the resilience ρ, the difference in the certainty equivalent ΔCE^{myo} decreases and ΔCE^{long} increases, respectively. This is because the price impact of frequent trading becomes less serious under a high market resilience. Hence, the investor should trade more aggressively towards the current Merton portfolio when ρ becomes larger. This can be seen from Figure 4(b): the aim portfolio of *opt* places more weights on the current Merton portfolio than the expected Merton portfolio for large ρ, leading our trading strategy to act more like *myo* than *long*. Thirdly, the outperformance of the optimal strategy is larger when the signal volatility β is larger,

since the signal fluctuates more significantly and it is more advantageous to aim in front of target rather than stick to either the current signal or only the long-run signal.

5. Conclusions

This paper studies optimal investment problems in the presence of both market illiquidity and return predictability. By capturing the three salient features of market liquidity – tightness, depth, and resilience – using a simple limit order book model, and the stochastic return-predicting signals using a mean-reversion process, we are able to achieve adequate tractability despite the high model dimensionality. In particular, we derive explicit optimal strategy in the base case with a constant return, and explicit asymptotic expansion under small signals in the general case with a stochastic return-predicting signal.

The tractable solutions developed in this paper casts managerial insights on the differentiated roles of market illiquidity and return predictability in investment decision making. We can encode the return predictability into the aim of the trading, which is based on a weighted average of the current return and the long-run return. On the other hand, the market illiquidity implies that one should pause trading and patiently wait for the future trading opportunities. *Patience indices* are established to quantify this timing decision. Our analysis demonstrates close relationship between the patience and the level of illiquidity. While these findings echoes the principle of "aiming in front of target" proposed in Gârleanu and Pedersen (2013, 2016), they illustrate how the principle works in a market with tightness and resilience: the virtue of patience lies in the timing of trading, rather than the smoothness of the trading.

Simulation based experiments further show that the advantages of our optimal strategy, measured by the certainty equivalences, are economically significant over strategies that disregard patience or ignore the dynamics of the return-predicting signal, in a wide range of market environments. Our model also leads to some testable implications that the trading volumes are positively correlated with the market resilience and depth.

Endnotes

1. Gârleanu and Pedersen (2013, 2016) take a reduced form approach to model market illiquidity by assuming quadratic transaction costs. Therefore, immediate round-trip trading is affordable in the presence of both transitory and persistent impact costs in their paper. See p. 499 of Gârleanu and Pedersen (2016) for more discussion.

References

Alfonsi, A., Fruth, A., and Schied, A. (2008). Constrained portfolio liquidation in a limit order book model. *Banach Center Publ*, 83:9–25.

Almgren, R. and Chriss, N. (2001). Optimal execution of portfolio transactions. *Journal of Risk*, 3:5–40.

Bank, P., Soner, H. M., and Voß, M. (2015). Hedging with transient price impact. *arXiv preprint arXiv:1510.03223*.

Bank, P., Soner, H. M., and Voß, M. (2017). Hedging with temporary price impact. *Mathematics and Financial Economics*, 11:215–239.

Bank, P. and Voß, M. (2019). Optimal investment with transient price impact. *SIAM Journal on Financial Mathematics*, 10(3):723–768.

Barberis, N. (2000). Investing for the long run when returns are predictable. *The Journal of Finance*, 55(1):225–264.

Bertsimas, D. and Lo, A. W. (1998). Optimal control of execution costs. *Journal of Financial Markets*, 1(1):1–50.

Biais, B., Hillion, P., and Spatt, C. (1995). An empirical analysis of the limit order book and the order flow in the paris bourse. *Journal of Finance*, 50(5):1655–1689.

Blais, M. and Protter, P. (2010). An analysis ff the supply curve for liquidity risk through book data. *International Journal of Theoretical and Applied Finance*, 13:1655–1689.

Bouchaud, J.-P., Farmer, J. D., and Lillo, F. (2009). How markets slowly digest changes in supply and demand. In *Handbook of Financial Markets: Dynamics and Evolution*, pages 57–160. Elsevier.

Brogaard, J., Hendershott, T., and Riordan, R. (2014). High-frequency trading and price discovery. *The Review of Financial Studies*, 27(8):2267–2306.

Brokmann, X., Itkin, D., Muhle-Karbe, J., and Schmidt, P. (2023). Tackling nonlinear price impact with linear strategies. *Available at SSRN: http://dx.doi.org/10.2139/ssrn.4584448*.

Cai, J., Chen, X., and Dai, M. (2018). Portfolio selection with capital gains tax, recursive utility, and regime switching. *Management Science*, 64(5):2308–2324.

Campbell, J. Y. and Viceira, L. M. (1999). Consumption and portfolio decisions when expected returns are time varying. *The Quarterly Journal of Economics*, 114(2):433–495.

Chen, X., Dai, M., Jiang, W., and Qin, C. (2022). Asymptotic analysis of long-term investment with two illiquid and correlated assets. *Mathematical Finance*, 32(4):1133–1169.

Dai, M., Jiang, L., Li, P., and Yi, F. (2009). Finite horizon optimal investment and consumption with transaction costs. *SIAM Journal on Control and Optimization*, 48(2):1134–1154.

Dai, M., Kou, S., Soner, H. M., and Yang, C. (2023). Leveraged exchange-traded funds with market closure and frictions. *Management Science*, 69(4):2517–2535.

Degryse, H., Jong, F. D., Ravenswaaij, M. V., and Wuyts, G. (2005). Aggressive orders and the resiliency of a limit order market. *Review of Finance*, 9(2):201–242.

Ekren, I. and Muhle-Karbe, J. (2019). Portfolio choice with small temporary and transient price impact. *Mathematical Finance*, 29(4):1066–1115.

Evans, L. C. (2002). *Partial Differential Equations*. American Mathematical Society, Providence, Rhode Island.

Fama, E. F. and French, K. R. (1988). Dividend yields and expected stock returns. *Journal of Financial Economics*, 22(1):3–25.

Ferson, W. E. and Harvey, C. R. (1993). The risk and predictability of international equity returns. *The Review of Financial Studies*, 6(3):527–566.

Gârleanu, N. and Pedersen, L. H. (2013). Dynamic trading with predictable returns and transaction costs. *The Journal of Finance*, 68(6):2309–2340.

Gârleanu, N. and Pedersen, L. H. (2016). Dynamic portfolio choice with frictions. *Journal of Economic Theory*, 165:487–516.

George, T. J. and Longstaff, F. A. (1993). Bid-ask spreads and trading activity in the s&p 100 index options market. *Journal of Financial and Quantitative Analysis*, 28(3):381–397.

Gould, M. D., Porter, M. A., Williams, S., McDonald, M., Fenn, D. J., and Howison, S. D. (2013). Limit order books. *Quantitative Finance*, 13(11):1709–1742.

Guasoni, P. and Weber, M. H. (2018). Rebalancing multiple assets with mutual price impact. *Journal of Optimization Theory and Applications*, 179:618–653.

Guasoni, P. and Weber, M. H. (2020). Nonlinear price impact and portfolio choice. *Mathematical Finance*, 30(2):341–376.

Hamao, Y. and Hasbrouck, J. (1995). Securities trading in the absence of dealers: Trades and quotes on the tokyo stock exchange. *The Review of Financial Studies*, 8(3):849–878.

Haugh, M. and Wang, C. (2014). Dynamic portfolio execution and information relaxations. *SIAM Journal on Financial Mathematics*, 5(1):316–359.

Horst, U. and Naujokat, F. (2014). When to cross the spread? trading in two-sided limit order books. *SIAM Journal on Financial Mathematics*, 5(1):278–315.

Johannes, M., Korteweg, A., and Polson, N. (2014). Sequential learning, predictability, and optimal portfolio returns. *The Journal of Finance*, 69(2):611–644.

Karatzas, I. and Shreve, S. E. (1991). *Brownian Motion and Stochastic Calculus*. Springer.

Kempf, A., Mayston, D., and Yadav, P. K. (2009). Resiliency in limit order book markets: A dynamic view of liquidity. In *AFA 2009 San Francisco Meetings Paper*, pages 1–39. Citeseer.

Kim, T. S. and Omberg, E. (1996). Dynamic nonmyopic portfolio behavior. *The Review of Financial Studies*, 9(1):141–161.

Koijen, R. S., Rodriguez, J. C., and Sbuelz, A. (2009). Momentum and mean reversion in strategic asset allocation. *Management Science*, 55(7):1199–1213.

Kyle, A. S. (1985). Continuous auctions and insider trading. *Econometrica: Journal of the Econometric Society*, pages 1315–1335.

Large, J. (2007). Measuring the resiliency of an electronic limit order book. *Journal of Financial Markets*, 10(1):1–25.

Lewis, C., Munyan, B., and Verwijmeren, P. (2023). Convertible debt arbitrage crashes revisited. *Journal of Financial and Quantitative Analysis*, pages 1–61.

Liu, H. (2004). Optimal consumption and investment with transaction costs and multiple risky assets. *The Journal of Finance*, 59(1):289–338.

Lo, D. K. and Hall, A. D. (2015). Resiliency of the limit order book. *Journal of Economic Dynamics and Control*, 61:222–244.

Markowitz, H. M. (1952). Portfolio selection. *Journal of Finance*, 7:77–91.

Merton, R. (1971). Optimum consumption and portfolio rules in a continuous-time model. *Journal of Economic Theory*, 3(4):373–413.

Merton, R. C. (1969). Lifetime portfolio selection under uncertainty: The continuous-time case. *The Review of Economics and Statistics*, pages 247–257.

Muhle-Karbe, J., Reppen, M., and Soner, H. M. (2017). A primer on portfolio choice with small transaction costs. *Annual Review of Financial Economics*, 9:301–331.

Muhle-Karbe, J., Sefton, J. A., and Shi, X. (2023a). Dynamic portfolio choice with intertemporal hedging and transaction costs. *Available at SSRN: http://dx.doi.org/10.2139/ssrn.4522752*.

Muhle-Karbe, J., Shi, X., and Yang, C. (2023b). An equilibrium model for the cross section of liquidity premia. *Mathematics of Operations Research*, 48(3):1423–1453.

Obizhaeva, A. A. and Wang, J. (2013). Optimal trading strategy and supply/demand dynamics. *Journal of Financial Markets*, 16(1):1–32.

Parlour, C. A. and Seppi, D. J. (2008). Limit order markets: A survey. *Handbook of Financial Intermediation and Banking*, 5:63–95.

Roch, A. and Soner, H. M. (2013). Resilient price impact of trading and the cost of illiquidity. *International Journal of Theoretical and Applied Finance*, 16(06):1350037.

Sharpe, W. F. (1964). Capital asset prices: A theory of market equilibrium under conditions of risk. *Journal of Finance*, 19:425–442.

Shreve, S. E. (2004). *Stochastic Calculus for Finance II: Continuous-Time Models*. Springer.

Shreve, S. E. and Soner, H. M. (1994). Optimal investment and consumption with transaction costs. *The Annals of Applied Probability*, pages 609–692.

Soner, H. M. and Touzi, N. (2013). Homogenization and asymptotics for small transaction costs. *Siam journal on control and optimization*, 51(4):2893–2921.

Soner, H. M. and Vukelja, M. (2016). Utility maximization in an illiquid market in continuous time. *Mathematical Methods of Operations Research*, 84:285–321.

Stein, E. M. and Shakarchi, R. (2009). *Real Analysis: Measure Theory, Integration, and Hilbert Spaces*. Princeton University Press.

Sun, L., Najand, M., and Shen, J. (2016). Stock return predictability and investor sentiment: A high-frequency perspective. *Journal of Banking & Finance*, 73:147–164.

Tsoukalas, G., Wang, J., and Giesecke, K. (2019). Dynamic portfolio execution. *Management Science*, 65(5):2015–2040.

Wachter, J. A. (2002). Portfolio and consumption decisions under mean-reverting returns: An exact solution for complete markets. *Journal of Financial and Quantitative Analysis*, 37(1):63–91.

Wang, G. H. and Yau, J. (2000). Trading volume, bid–ask spread, and price volatility in futures markets. *Journal of Futures Markets: Futures, Options, and Other Derivative Products*, 20(10):943–970.

Electronic Companion

EC.1.   The Viscosity Characterization of the Value Function

In this section, we prove that the value function V^ε given in (24) satisfies the HJB equation (25) in the viscosity sense. The baseline case in Section 3.1 corresponds to $\varepsilon = 0$. Furthermore, for the baseline case, we will derive the analytic form in Section EC.2, and therefore the value function satisfies the HJB equation in the classical sense. For the ease of notation, we suppress the superscript and use V in place of V^ε.

Lemma EC.1.1 *For any $t < T$, the value function V^ε satisfies the variational inequality* (25).

In the following, we denote

$$\mathcal{B}V = \frac{1}{q_a}\frac{\partial V}{\partial d_a} + \frac{\partial V}{\partial x} - (s + d_a)\frac{\partial V}{\partial y},$$
$$\mathcal{S}V = \frac{1}{q_b}\frac{\partial V}{\partial d_b} - \frac{\partial V}{\partial x} + (s - d_b)\frac{\partial V}{\partial y}.$$

Therefore, (25) is equivalent to

$$\min\left\{-\mathcal{L}^\varepsilon V, \ -\mathcal{B}V, \ -\mathcal{S}V\right\} = 0. \tag{EC.1}$$

The remaining of this section provides the proof of Lemma EC.1.1.

Let $K^0 = (t^0, s^0, \mu^0, x^0, y^0, d^{A,0}, d^{B,0}) \in [0, T] \times \mathcal{D}$.

EC.1.1.   Viscosity Subsolution

First we prove that V is a viscosity subsolution of (EC.1). In order to prove this, we need to show that for all smooth function $\varphi(K)$, such that $V(K) - \varphi(K)$ has a local maximum at K^0, the following inequality holds

$$\min\left\{-\mathcal{L}^\varepsilon\varphi(K^0), \ -\mathcal{B}\varphi(K^0), \ -\mathcal{S}\varphi(K^0)\right\} \leq 0. \tag{EC.2}$$

Without loss of generality, we assume that $V(K^0) = \varphi(K^0)$ and $V \leq \varphi$ on $[0, T] \times \mathcal{D}$. We argue by contradiction and suppose that the arguments inside the minimum operator of the inequality (EC.2) satisfy

$$\mathcal{B}\varphi(K^0) < 0, \ \ \mathcal{S}\varphi(K^0) < 0,$$

and there exists $\theta > 0$ such that

$$\mathcal{L}\varphi(K^0) < -\theta.$$

ec1

Since φ is smooth, the above inequalities become

$$\mathcal{B}\varphi(K) < 0, \quad \mathcal{S}\varphi(K) < 0, \quad \mathcal{L}\varphi(K) \leq -\theta, \tag{EC.3}$$

where $K = (t, s, \mu, x, y, d_a, d_b) \in \mathcal{N}(K^0)$, a neighbourhood of K^0. Let $\{h_m\}$ be a positive sequence such that $h_m \to 0$ as m goes to infinity. Define

$$\tau(\omega) := \inf\{t \in [t^0, T] : K_t^{0,\wedge} \notin \mathcal{N}(K^0)\},$$

and it is positive $\mathbb{P}$-a.s.. Let $\tau_m := \tau \wedge h_m$, then there exists a pair of $\{L_t^\wedge, M_t^\wedge\}$ such that

$$\varphi(K^0) - \frac{\theta h_m}{2} \leq \mathbb{E}[\varphi(K_{\tau_m}^{0,\wedge})].$$

where $K_t^{0,\wedge}$ is the state trajectory under the strategy $\{L_t^\wedge, M_t^\wedge\}$. Applying Ito's formula to $\varphi(K)$, we can obtain

$$-\frac{\theta h_m}{2} - \mathbb{E}\Big[\int_{t_0}^{\tau_m} \mathcal{B}\varphi(K_t^{0,\wedge})\mathrm{d}L_t^\wedge\Big] - \mathbb{E}\Big[\int_{t_0}^{\tau_m} \mathcal{S}\varphi(K_t^{0,\wedge})\mathrm{d}M_t^\wedge\Big] - \mathbb{E}\Big[\int_{t_0}^{\tau_m} \mathcal{L}^\varepsilon\varphi(K_t^{0,\wedge})\mathrm{d}t\Big] \leq 0 \text{(EC.4)}$$

Using the inequalities (EC.3), we have

$$-\frac{\theta h_m}{2} - \mathbb{E}\Big[\int_{t_0}^{\tau_m} \mathcal{B}\varphi(K_t^{0,\wedge})\mathrm{d}L_t^\wedge\Big] - \mathbb{E}\Big[\int_{t_0}^{\tau_m} \mathcal{S}\varphi(K_t^{0,\wedge})\mathrm{d}M_t^\wedge\Big] - \mathbb{E}\Big[\int_{t_0}^{\tau_m} \mathcal{L}^\varepsilon\varphi(K_t^{0,\wedge})\mathrm{d}t\Big]$$
$$> -\frac{\theta h_m}{2} + \theta\mathbb{E}[\tau_m]. \tag{EC.5}$$

Since τ is positive $\mathbb{P}$-a.s., and $h_m \to 0$ as $m \to \infty$, we have $\mathbb{E}[\tau_m] \to h_m$ as $m \to \infty$. Therefore, the right-hand side of (EC.5) is strictly positive. Then there is a contradiction between (EC.4) and (EC.5). Therefore at least one argument inside the minimum operator is nonpositive, and the inequality (EC.2) holds. Then the value function V is a viscosity subsolution of the variational inequality (EC.1).

EC.1.2. Viscosity Supersolution

Then we prove that V is a viscosity supersolution of (EC.1). In order to prove this, we need to show that for all smooth function $\varphi(K)$, such that $V(K) - \varphi(K)$ has a local minimum at K^0, the following inequality holds

$$\min\Big\{-\mathcal{L}^\varepsilon\varphi(K^0), \quad -\mathcal{B}\varphi(K^0), \quad -\mathcal{S}\varphi(K^0)\Big\} \geq 0. \tag{EC.6}$$

Without loss of generality, we assume that $V(K^0) = \varphi(K^0)$ and $V \geq \varphi$ on $[0, T] \times \mathcal{D}$. We need to prove each argument inside the minimum operator of (EC.6) is nonnegative.

Consider the trading strategy $\Delta L_{t^0} = \xi > 0$, $\Delta M_{t^0} = 0$ and $\mathrm{d}L_t = \mathrm{d}M_t = 0$ for $t^0 < t \leq T$. From the dynamic programming principle, we have

$$V(t^0, s^0, \mu^0, x^0, y^0, d^{A,0}, d^{B,0}) \geq V(t^0, s^0, \mu^0, x^0 + \xi, y^0 - (s^0 + d^{A,0})\xi - \frac{1}{2q_a}\xi^2, d^{A,0} + \frac{1}{q_a}\xi, d^{B,0}).$$

ec2

Since $V(K^0) = \varphi(K^0)$, and $V(K) \geq \varphi(K)$ for any K, we see that this inequality also holds for $\varphi(t, s, \mu, x, y, d_a, d_b)$, i.e.,

$$\varphi(t^0, s^0, \mu^0, x^0, y^0, d^{A,0}, d^{B,0}) \geq \varphi(t^0, s^0, \mu^0, x^0 + \xi, y^0 - (s^0 + d^{A,0})\xi - \frac{1}{2q_a}\xi^2, d^{A,0} + \frac{1}{q_a}\xi, d^{B,0}).$$

Then subtracting the left-hand side from the right-hand side of this inequality, dividing by ξ and letting $\xi \to 0$, we have

$$\mathcal{B}\varphi(K^0) = \frac{1}{q_a}\frac{\partial\varphi(K^0)}{\partial d_a} + \frac{\partial\varphi(K^0)}{\partial x} - (s^0 + d^{A,0})\frac{\partial\varphi(K^0)}{\partial y} \leq 0.$$

Similarly, consider the trading strategy $\Delta L_{t^0} = 0$, $\Delta M_{t^0} = \xi > 0$ and $\mathrm{d}L_t = \mathrm{d}M_t = 0$ for $t^0 < t \leq T$, we have

$$\mathcal{S}\varphi(K^0) = \frac{1}{q_b}\frac{\partial\varphi(K^0)}{\partial d_b} - \frac{\partial\varphi(K^0)}{\partial x} + (s^0 - d^{B,0})\frac{\partial\varphi(K^0)}{\partial y} \leq 0.$$

Then consider the case with no trade, i.e., $\mathrm{d}L_t = \mathrm{d}M_t = 0$ for $t^0 \leq t \leq T$. From the dynamic programming principle, we have

$$V(t^0, s^0, \mu^0, x^0, y^0, d^{A,0}, d^{B,0}) \geq \mathbb{E}[V(K_t^{0,d})],$$

where $K_t^{0,d}$ is the state trajectory when $L_t = M_t = 0$ for $t^0 \leq t \leq T$, i.e.,

$$K_t^{0,d} = \Big(t,\ s^0 + \int_{t^0}^t \mu_u du + \sigma(W_t - W_{t^0}),\ \mu^0 e^{-\varepsilon b(t-t^0)} + \frac{a}{b}(1 - e^{-\varepsilon b(t-t^0)}) + \varepsilon\beta \int_{t^0}^t e^{-\varepsilon b(t-u)} dW'_u,$$
$$x^0,\ y^0,\ d^{A,0}e^{-\rho_a(t-t^0)},\ d^{B,0}e^{-\rho_b(t-t^0)}\Big),$$

and $K_t^{0,d} \in \mathcal{N}(K^0)$. This inequality also holds for $\varphi(t, S, \mu, X, Y, D^a, D^b)$. Applying Ito's formula to $\varphi(K)$, we can obtain

$$\mathbb{E}\Big[\int_{t^0}^t \Big(\frac{\partial\varphi(K_u^{0,d})}{\partial t} + \mu_u^{0,d}\frac{\partial\varphi(K_u^{0,d})}{\partial s} + \frac{1}{2}\sigma^2\frac{\partial^2\varphi(K_u^{0,d})}{\partial s^2} + \varepsilon(a - b\mu_u^{0,d})\frac{\partial\varphi(K_u^{0,d})}{\partial\mu} + \frac{1}{2}\varepsilon^2\beta^2\frac{\partial^2\varphi(K_u^{0,d})}{\partial\mu^2}$$
$$- \rho_a D_u^{A,0,d}\frac{\partial\varphi(K_u^{0,d})}{\partial d_a} - \rho_b D_u^{B,0,d}\frac{\partial\varphi(K_u^{0,d})}{\partial d_b}\Big) du\Big] \leq 0.$$

Let $t \to t^0$, we have

$$\mathcal{L}^\varepsilon\varphi(K^0) = \frac{\partial\varphi(K^0)}{\partial t} + \mu^0\frac{\partial\varphi(K^0)}{\partial s} + \frac{1}{2}\sigma^2\frac{\partial^2\varphi(K^0)}{\partial s^2} + \varepsilon(a - b\mu^0)\frac{\partial\varphi(K^0)}{\partial\mu} + \frac{1}{2}\varepsilon^2\beta^2\frac{\partial^2\varphi(K^0)}{\partial\mu^2}$$
$$- \rho_a d^{A,0}\frac{\partial\varphi(K^0)}{\partial d_a} - \rho_b d^{B,0}\frac{\partial\varphi(K^0)}{\partial d_b} \leq 0.$$

Therefore all the three arguments inside the minimum operator are nonnegative, and the inequality (EC.6) holds. Then the value function V is a viscosity supersolution of the variational inequality (EC.1). Q.E.D.

ec3

EC.2. Proof of Theorem 3.1

The proofs related to Theorem 3.1 are laid out in the four parts in this section.

EC.2.1. Variational Inequality

Let $\varepsilon = 0$. Due to the property of the exponential utility function, we can reduce the dimension of this problem. Let $V(t, s, x, y, d_a, d_b) = 1 - \exp\left\{ -\gamma \left[y + sx + F(t, x, d_a, d_b) \right] \right\}$. Then, from (25), F corresponds to the equation

$$\max\left\{ \widetilde{\mathcal{L}}F, \quad \frac{1}{q_a}\frac{\partial F}{\partial d_a} + \frac{\partial F}{\partial x} - d_a, \quad \frac{1}{q_b}\frac{\partial F}{\partial d_b} - \frac{\partial F}{\partial x} - d_b \right\} = 0, \qquad (\text{EC.7})$$

where

$$\widetilde{\mathcal{L}}F := \frac{\partial F}{\partial t} - \rho_a d_a \frac{\partial F}{\partial d_a} - \rho_b d_b \frac{\partial F}{\partial d_b} - \frac{1}{2}\sigma^2\gamma(x - \frac{\mu}{\sigma^2\gamma})^2 + \frac{\mu^2}{2\sigma^2\gamma},$$

with $F(T, x, d_a, d_b) = 0$.

Lemma EC.2.1 *The explicit form of $F(t, x, d_a, d_b)$ is given by*

- *if $x \geq \frac{\mu}{\sigma^2\gamma} + h_b(t)d_b$, then*

$$F(t, x, d_a, d_b) = \frac{\mu^2}{2\sigma^2\gamma}(T - t) + f_b(t)(x - \frac{\mu}{\sigma^2\gamma} + q_b d_b)^2 + \frac{q_b}{2}(d_b)^2;$$

- *if $x \leq \frac{\mu}{\sigma^2\gamma} - h_a(t)d_a$, then*

$$F(t, x, d_a, d_b) = \frac{\mu^2}{2\sigma^2\gamma}(T - t) + f_a(t)(x - \frac{\mu}{\sigma^2\gamma} - q_a d_a)^2 + \frac{q_a}{2}(d_a)^2;$$

- *if $\frac{\mu}{\sigma^2\gamma} + \frac{\rho_b}{\sigma^2\gamma}e^{-\rho_b(T - \frac{1}{\rho_b} - t)}d_b < x < \frac{\mu}{\sigma^2\gamma} + h_b(t)d_b$ and $t < T - \frac{1}{\rho_b}$, then*

$$F(t, x, d_a, d_b) = \frac{\mu^2}{2\sigma^2\gamma}(T - t) + f_b(\tau_b)(x - \frac{\mu}{\sigma^2\gamma} + q_b e^{-\rho_b(\tau_b - t)}d_b)^2$$
$$- \frac{1}{2}\sigma^2\gamma(\tau_b - t)(x - \frac{\mu}{\sigma^2\gamma})^2 + \frac{q_b}{2}e^{-2\rho_b(\tau_b - t)}(d_b)^2;$$

- *if $\frac{\mu}{\sigma^2\gamma} - h_a(t)d_a < x < \frac{\mu}{\sigma^2\gamma} - \frac{\rho_a}{\sigma^2\gamma}e^{-\rho_a(T - \frac{1}{\rho_a} - t)}d_a$ and $t < T - \frac{1}{\rho_a}$, then*

$$F(t, x, d_a, d_b) = \frac{\mu^2}{2\sigma^2\gamma}(T - t) + f_a(\tau_a)(x - \frac{\mu}{\sigma^2\gamma} - q_a e^{-\rho_a(\tau_a - t)}d_a)^2$$
$$- \frac{1}{2}\sigma^2\gamma(\tau_a - t)(x - \frac{\mu}{\sigma^2\gamma})^2 + \frac{q_a}{2}e^{-2\rho_a(\tau_a - t)}(d_a)^2;$$

- *otherwise,*

$$F(t, x, d_a, d_b) = \frac{\mu^2}{2\sigma^2\gamma}(T - t) - \frac{1}{2}\sigma^2\gamma(T - t)(x - \frac{\mu}{\sigma^2\gamma})^2.$$

ec4

In the above, τ_a is given by $x - \frac{\mu}{\sigma^2\gamma} - h_b(\tau_b)e^{-\rho_b(\tau_b-t)}d_b = 0$, and τ_a is given by $x - \frac{\mu}{\sigma^2\gamma} + h_a(\tau_a)e^{-\rho_a(\tau_a-t)}d_a = 0$.

Furthermore, the boundaries of the buy and sell regions correspond to

$$x - \frac{\mu}{\sigma^2\gamma} + h_a(t)d_a = 0 \ \text{ and } \ x - \frac{\mu}{\sigma^2\gamma} - h_b(t)d_b = 0,$$

respectively, where for $i = a, b$,

$$h_i(t) = \begin{cases} \frac{q_i(\rho_i f_i(t) - f_i'(t))}{f_i'(t) - \frac{1}{2}\sigma^2\gamma}, & \text{if } t < T - \frac{1}{\rho_i} \\[2ex] \frac{1}{\sigma^2\gamma(T-t)}, & \text{if } t \geq T - \frac{1}{\rho_i} \end{cases} \tag{EC.8}$$

with

$$f_i(t) = \frac{\frac{2\rho_i}{q_i} + \sigma^2\gamma}{2\rho_i^2}\left[\frac{R_i}{2} + \eta_i \frac{(1+\xi_i)e^{-\eta_i(T-\frac{1}{\rho_i}-t)} - (1-\xi_i)e^{\eta_i(T-\frac{1}{\rho_i}-t)}}{(1+\xi_i)e^{-\eta_i(T-\frac{1}{\rho_i}-t)} + (1-\xi_i)e^{\eta_i(T-\frac{1}{\rho_i}-t)}}\right], \tag{EC.9}$$

$$R_i = \frac{2\rho_i\sigma^2\gamma}{\frac{2\rho_i}{q_i} + \sigma^2\gamma}, \quad s_i = -\frac{2\rho_i^3 \frac{1}{q_i}\sigma^2\gamma}{(\frac{2\rho_i}{q_i} + \sigma^2\gamma)^2}, \quad \eta_i = \sqrt{\frac{R_i^2}{4} - s_i} = \sqrt{\frac{\rho_i^2\sigma^2\gamma}{\frac{2\rho_i}{q_i} + \sigma^2\gamma}}, \quad \xi_i = -\frac{\sqrt{\sigma^2\gamma(\frac{2\rho_i}{q_i} + \sigma^2\gamma)}}{\frac{\rho_i}{q_i} + \sigma^2\gamma}.$$

Lemma EC.2.1 can be verified via direct calculations.

EC.2.2. Verification Principle

Denote $V(t, s, x, y, d_a, d_b)$ as the value function and $J(t, s, x, y, d_a, d_b)$ as the cost functional for any given feasible policy $\{L_t, \ M_t: \ 0 \leq t \leq T\}$. For any $\tau \in [t, T]$, denote $J_\tau(t, s, x, y, d_a, d_b)$ as the cost functional for an policy which follows $\{L_t, \ M_t: \ 0 \leq t \leq T\}$ on $[t, \tau]$ and $\{L_t^*, \ M_t^*: \ 0 \leq t \leq T\}$ on $[\tau, T]$. Then

$$\begin{aligned} &J_\tau(t, s, x, y, d_a, d_b) \\ &= \mathbb{E}_t[V(\tau, S_\tau, X_\tau, Y_\tau, D_\tau^a, D_\tau^b)] \\ &= V(t, s, x, y, d_a, d_b) + \mathbb{E}_t\Big[\int_t^\tau V_u du + \int_t^\tau V_s dS + \int_t^\tau V_x dX + \int_t^\tau V_y dY \\ &\quad + \int_t^\tau V_{d_a} dd_a + \int_t^\tau V_{d_b} dd_b + \frac{1}{2}\int_t^\tau V_{ss} d[S, S] + \sum_{t \leq u \leq \tau} \Delta V\Big] \\ &= V(t, s, x, y, d_a, d_b) \\ &\quad + \mathbb{E}_t\Big[\int_t^\tau (V_u + \mu V_s + \frac{1}{2}\sigma^2 V_{ss} - \rho_a d_a V_{d_a} - \rho_b d_b V_{d_b}) du\Big] \\ &\quad + \mathbb{E}_t\Big[\int_t^\tau \big(V_x - (s + d_a)V_y + \frac{1}{q_a}V_{d_a}\big)l du\Big] \\ &\quad + \mathbb{E}_t\Big[\int_t^\tau \big(-V_x + (s - d_b)V_y + \frac{1}{q_b}V_{d_b}\big)m du\Big] + \mathbb{E}_t\Big[\sum_{t \leq u \leq \tau} \Delta V\Big] \\ &\leq V(t, s, x, y, d_a, d_b) \end{aligned}$$

ec5

where

$$\sum_{t \le u \le \tau} \Delta V = \sum_{t \le u \le \tau} \Big[V\big(u, S_u, X_{u-} + \Delta L_u, Y_{u-} - (S_u + D_{u-}^a)\Delta L_u - \frac{1}{2q_a}(\Delta L_u)^2, D_{u-}^a + \frac{1}{q_a}\Delta L_u, D_u^b\big)$$

$$+ V\big(u, S_u, X_{u-} - \Delta M_u, Y_{u-} + (S_u - D_{u-}^b)\Delta M_u - \frac{1}{2q_b}(\Delta M_u)^2, D_u^a, D_{u-}^b + \frac{1}{q_b}\Delta M_u\big)$$

$$- V(u-, S_{u-}, X_{u-}, Y_{u-}, D_{u-}^a, D_{u-}^b)\Big].$$

The first three integrals are less than or equal to 0 because of the variational inequality, the summation is 0 because the value doesn't change before and after the jump.

The value change of the jump part is 0 can be verified by the explicit expression of the value function in the trading region. Suppose the initial state is in the sell region, and the magnitude of jump sale is ξ. Then

$$V(t, S_t, X_t, Y_t, D_t^a, D_t^b)$$

$$= V(t, S_t, X_{t-} - \xi, Y_{t-} + (S_t - D_{t-}^b)\xi - \frac{1}{2q}\xi^2, D_t^a, D_{t-}^b + \frac{1}{q}\xi)$$

$$= 1 - \exp\{-\gamma[Y_{t-} + (S_t - D_{t-}^b)\xi - \frac{1}{2q}\xi^2 + S_t(X_{t-} - \xi) + \frac{q}{2}(D_{t-}^b + \frac{1}{q}\xi)^2$$

$$+ f_0(t)\big(X_{t-} - \xi - \frac{\mu}{\sigma^2\gamma} + q(D_{t-}^b + \frac{1}{q}\xi)\big)^2 + \frac{\mu^2}{\sigma^2\gamma}(T - t)]\}$$

$$= 1 - \exp\{-\gamma[Y_{t-} + S_t X_{t-} + \frac{q}{2}(D_{t-}^b)^2 + f_0(t)(X_{t-} - \frac{\mu}{\sigma^2\gamma} + q D_{t-}^b)^2 + \frac{\mu^2}{2\sigma^2\gamma}(T - t)]\}$$

$$= V(t-, S_{t-}, X_{t-}, Y_{t-}, D_{t-}^a, D_{t-}^b)$$

Let $\tau \to t$, then $J(t, s, x, y, d_a, d_b) \le V(t, s, x, y, d_a, d_b)$, equality holds if $\{L_t,\ M_t:\ 0 \le t \le T\} = \{L_t^*,\ M_t^*:\ 0 \le t \le T\}$.

EC.2.3. Optimal Dynamic Trading Strategy

Finally, we establish (17) – (19). Recall that the sell boundary is given by $x = \frac{\mu}{\sigma^2\gamma} + h(t)d_b$. Then given the initial state x and d_b satisfying $x > \frac{\mu}{\sigma^2\gamma} + h(t)d_b$, there will be an initial jump sale to the sell boundary, which satisfies $X_t = \frac{\mu}{\sigma^2\gamma} + h(t)D_t^b$ with $X_t = x - \Delta M_t$ and $D_t^b = d_b + \frac{1}{q}\Delta M_t$. So the initial jump sale is

$$\Delta M_t = \frac{x - \frac{\mu}{\sigma^2\gamma} - h(t)d_b}{1 + \frac{1}{q}h(t)}.$$

Then the investor will pursue continuous selling at the rate m_u ($t \le u \le T - \frac{1}{\rho}$) to make sure going along the sell boundary. The rate m_u can be determined by taking derivatives to the boundary and substituting the dynamics of X_u and D_u^b into the expression, and we can express it as

$$m_u = \frac{\rho h(u) - h'(u)}{1 + \frac{1}{q}h(u)}D_u^b = \frac{\rho h(u) - h'(u)}{h(u)(1 + \frac{1}{q}h(u))}(X_u - \frac{\mu}{\sigma^2\gamma}).$$

ec6

It is equivalent to

$$\frac{dX_u}{du} + \frac{\rho h(u) - h'(u)}{h(u)(1 + \frac{1}{q}h(u))}(X_u - \frac{\mu}{\sigma^2\gamma}) = 0, \tag{EC.10}$$

which is a first-order linear ODE with initial condition $X_t = x - \Delta M_t = \frac{\frac{1}{q}h(t)x + \frac{\mu}{\sigma^2\gamma} + h(t)d_b}{1 + \frac{1}{q}h(t)}$ and thus we can solve X_u for $t \le u \le T - \frac{1}{\rho}$. Then let $m_u = -\frac{dX_u}{du}$ to obtain the explicit expression of m_u using the initial state.

Furthermore, taking derivatives once more, we can obtain

$$\frac{d^2X_u}{du^2} + s(u)\frac{dX_u}{du} + s'(u)(X_u - \frac{\mu}{\sigma^2\gamma}) = 0, \tag{EC.11}$$

where $s(u) = \frac{\rho h(u) - h'(u)}{h(u)(1 + \frac{1}{q}h(u))}$ and $s'(u) = -\frac{\frac{\rho}{q}h^2(u)h'(u) + h(u)h''(u) + \frac{1}{q}h^2(u)h''(u) - h'^2(u) - \frac{2}{q}h(u)h'^2(u)}{h^2(u)(1 + \frac{1}{q}h(u))^2}$. Then substituting (EC.10) into (EC.11), we can derive

$$\frac{d^2X_u}{du^2} = (s^2(u) - s'(u))(X_u - \frac{\mu}{\sigma^2\gamma}).$$

Using the explicit expression of the function $h(u)$, we can calculate that $s^2(u) - s'(u) = \frac{\rho^2\sigma^2\gamma}{\frac{2\rho}{q} + \sigma^2\gamma} = \eta^2$ holds true for all $t \le u \le T - \frac{1}{\rho}$. So the optimal shares holding X_u ($t \le u \le T - \frac{1}{\rho}$) satisfies the constant coefficient second-order linear ODE

$$\frac{d^2X_u}{du^2} = \frac{\rho^2\sigma^2\gamma}{\frac{2\rho}{q} + \sigma^2\gamma}(X_u - \frac{\mu}{\sigma^2\gamma}),$$

with initial conditions

$$\begin{cases} X_t = x - \Delta M_t = \frac{\frac{1}{q}h(t)x + \frac{\mu}{\sigma^2\gamma} + h(t)d_b}{1 + \frac{1}{q}h(t)} := z_1(t, x, d_b), \\[2mm] \frac{dX_u}{du}\big|_{u=t} = \frac{\rho h(t) - h'(t)}{h(t)(1 + \frac{1}{q}h(t))}\left(\frac{\mu}{\sigma^2\gamma} - \frac{\frac{1}{q}h(t)x + \frac{\mu}{\sigma^2\gamma} + h(t)d_b}{1 + \frac{1}{q}h(t)}\right) := z_2(t, x, d_b). \end{cases}$$

The solution to the above ODE has the form $X_u = c_1 e^{\eta u} + c_2 e^{-\eta u} + \frac{\mu}{\sigma^2\gamma}$. Using the initial conditions, we can solve $c_1 = \frac{1}{2}(z_1 + \frac{1}{\eta}z_2 - \frac{\mu}{\sigma^2\gamma})e^{-\eta t}$ and $c_2 = \frac{1}{2}(z_1 - \frac{1}{\eta}z_2 - \frac{\mu}{\sigma^2\gamma})e^{\eta t}$.   Q.E.D.

EC.3.   Proof of Eq. (22)

We omit the subscript a or b in the following proof. From the expression of $h(t)$ in (EC.8), and let $\phi = \frac{\frac{2\rho}{q} + \sigma^2\gamma}{\sigma^2\gamma\rho}\eta$, we can directly calculate

$$\frac{h'(t)}{h(t)} - \rho$$

$$= \frac{-4\rho(1 - \xi^2)}{[(1+\xi)e^{-\eta(T - \frac{1}{\rho} - t)} - (1-\xi)e^{\eta(T - \frac{1}{\rho} - t)}][(\phi+1)(1+\xi)e^{-\eta(T - \frac{1}{\rho} - t)} + (\phi-1)(1-\xi)e^{\eta(T - \frac{1}{\rho} - t)}]} - \rho$$

$$= \frac{-4\rho(1 - \xi^2)}{(1+\phi)(1+\xi)^2 e^{-2\eta(T - \frac{1}{\rho} - t)} - 2(1-\xi^2) + (1-\phi)(1-\xi)^2 e^{2\eta(T - \frac{1}{\rho} - t)}} - \rho,$$

ec7

with $-1 < \xi < 0$ and $\phi > 1$.

Let $\delta(t) = (1+\phi)(1+\xi)^2 e^{-2\eta(T-\frac{1}{\rho}-t)} - 2(1-\xi^2) + (1-\phi)(1-\xi)^2 e^{2\eta(T-\frac{1}{\rho}-t)}$, then

$$\delta'(t) = 2\eta(1+\phi)(1+\xi)^2 e^{-2\eta(T-\frac{1}{\rho}-t)} - 2\eta(1-\phi)(1-\xi)^2 e^{2\eta(T-\frac{1}{\rho}-t)} > 0,$$

which implies $\delta(t)$ increases with t. Then $\frac{h'(t)}{h(t)} - \rho$ is also an increasing function with respect to time t. By some direct calculations, we derive that at time $t = T - \frac{1}{\rho}$,

$$\frac{h'(T-\frac{1}{\rho})}{h(T-\frac{1}{\rho})} - \rho = \frac{-4\rho(1-\xi^2)}{4\xi(\xi+\phi)} - \rho = -\frac{\rho(\rho+\sigma^2\gamma q)}{2\rho+\sigma^2\gamma q} < 0.$$

So we have $\frac{h'(t)}{h(t)} - \rho < 0$ holds true for any $0 \le t < T - \frac{1}{\rho}$, which proves the proposition.

Q.E.D.

EC.4. Proof of Theorem 3.2

The proof follows the idea in Soner and Touzi (2013), Muhle-Karbe et al. (2017). Due to the property of the exponential utility function and the independence of the two Brownian motions W and W', we can still reduce the dimension of this problem. Let $V(t,s,\mu,x,y,d_a,d_b) = 1 - \exp\{-\gamma[y + sx + F(t,\mu,x,d_a,d_b)]\}$, and the optimal value function F satisfies the following variational inequality

$$\max\{\mathcal{L}_F^\varepsilon F, \quad \mathcal{B}_F F, \quad \mathcal{S}_F F\} = 0, \tag{EC.12}$$

where

$$\mathcal{L}_F^\varepsilon F = \frac{\partial F}{\partial t} + \mu x - \frac{1}{2}\sigma^2\gamma x^2 + \varepsilon\kappa(\bar\mu - \mu)\frac{\partial F}{\partial\mu} + \frac{1}{2}\varepsilon^2\beta^2\Big[\frac{\partial^2 F}{\partial\mu^2} - \gamma(\frac{\partial F}{\partial\mu})^2\Big] - \rho_a d_a\frac{\partial F}{\partial d_a} - \rho_b d_b\frac{\partial F}{\partial d_b},$$

$$\mathcal{B}_F F = \frac{1}{q_a}\frac{\partial F}{\partial d_a} + \frac{\partial F}{\partial x} - d_a,$$

$$\mathcal{S}_F F = \frac{1}{q_b}\frac{\partial F}{\partial d_b} - \frac{\partial F}{\partial x} - d_b,$$

with $F(T,\mu,x,d_a,d_b) = 0$. We can reformulate (EC.12) as the following free-boundary problem for F with the unknown no-trade region $\mathcal{NR}^\varepsilon$ and the unknown optimal trading boundaries $\partial\mathcal{NR}^\varepsilon$ such that

$$\begin{cases} \frac{\partial F}{\partial t} + \mu x - \frac{1}{2}\sigma^2\gamma x^2 + \varepsilon\kappa(\bar\mu - \mu)\frac{\partial F}{\partial\mu} + \frac{1}{2}\varepsilon^2\beta^2[\frac{\partial^2 F}{\partial\mu^2} - \gamma(\frac{\partial F}{\partial\mu})^2] - \rho_a d_a\frac{\partial F}{\partial d_a} - \rho_b d_b\frac{\partial F}{\partial d_b} = 0 & \text{in } \mathcal{NR}^\varepsilon, \\[2mm] \frac{1}{q_a}\frac{\partial F}{\partial d_a} + \frac{\partial F}{\partial x} - d_a = 0, \quad \frac{1}{q_b}\frac{\partial F}{\partial d_b} - \frac{\partial F}{\partial x} - d_b = 0 & \text{on } \partial\mathcal{NR}^\varepsilon, \\[2mm] F(T,\mu,x,d_a,d_b) = 0. \end{cases} \tag{EC.13}$$

We solve (EC.12) piece by piece. Let

$$t_{0,i} = T - \frac{1}{\rho_i} + O(\varepsilon), \ i = a, b.$$

ec8

Focus on the state region in which $t \geq \max\{t_{0,a}, t_{0,b}\}$. For

$$\frac{\mu}{\sigma^2\gamma} - \frac{d_a}{\sigma^2\gamma(T-t)} + \frac{\kappa(T-t)}{2\sigma^2\gamma}(\bar{\mu}-\mu)\varepsilon + O(\varepsilon^2) < x < \frac{\mu}{\sigma^2\gamma} + \frac{d_b}{\sigma^2\gamma(T-t)} + \frac{\kappa(T-t)}{2\sigma^2\gamma}(\bar{\mu}-\mu)\varepsilon + O(\varepsilon^2),$$

define

$$F(t,\mu,x,d_a,d_b) = sx + \big(c_1(t;\varepsilon)\mu + c_2(t;\varepsilon)\big)x - \frac{1}{2}c_3(t;\varepsilon)x^2,$$

with

$$c_1(t;\varepsilon) = (T-t) - \frac{1}{2}\kappa(T-t)^2\varepsilon + \frac{1}{6}\kappa^2(T-t)^3\varepsilon^2 + O(\varepsilon^3),$$

$$c_2(t;\varepsilon) = \frac{1}{2}\kappa\bar{\mu}(T-t)^2\varepsilon - \frac{1}{6}\kappa^2\bar{\mu}(T-t)^3\varepsilon^2 + O(\varepsilon^3)$$

and $c_3(t;\varepsilon) = \sigma^2\gamma(T-t) + \frac{1}{3}\beta^2\gamma(T-t)^3\varepsilon^2 + O(\varepsilon^3)$. For

$$x > \frac{\mu}{\sigma^2\gamma} + \frac{d_b}{\sigma^2\gamma(T-t)} + \frac{\kappa(T-t)}{2\sigma^2\gamma}(\bar{\mu}-\mu)\varepsilon + O(\varepsilon^2), \tag{EC.14}$$

define

$$F(t,\mu,x,d_a,d_b) = sx + \frac{q_b}{2}d_b^2 - \frac{\sigma^2\gamma(T-t)}{2(1+\sigma^2\gamma q_b(T-t))}\Big(x + q_b d_b - \frac{\mu}{\sigma^2\gamma}\Big)^2 + \frac{\mu^2(T-t)}{2\sigma^2\gamma}$$
$$+ \frac{\kappa(T-t)^2}{2(1+\sigma^2\gamma q(T-t))}\Big[x + q_b d_b + q_b(T-t)\mu\Big](\bar{\mu}-\mu)\varepsilon + O(\varepsilon^2).$$

And for

$$x < \frac{\mu}{\sigma^2\gamma} - \frac{d_a}{\sigma^2\gamma(T-t)} + \frac{\kappa(T-t)}{2\sigma^2\gamma}(\bar{\mu}-\mu)\varepsilon + O(\varepsilon^2), \tag{EC.15}$$

define

$$F(t,\mu,x,d_a,d_b) = sx + \frac{q_a}{2}d_a^2 - \frac{\sigma^2\gamma(T-t)}{2(1+\sigma^2\gamma q_a(T-t))}\Big(x - q_a d_a - \frac{\mu}{\sigma^2\gamma}\Big)^2 + \frac{\mu^2(T-t)}{2\sigma^2\gamma}$$
$$+ \frac{\kappa(T-t)^2}{2(1+\sigma^2\gamma q_a(T-t))}\Big[x - q_a d_a + q_a(T-t)\mu\Big](\bar{\mu}-\mu)\varepsilon + O(\varepsilon^2).$$

It is straightforward to verify the above F, along with the boundaries defined in (EC.14) and (EC.15), satisfies the equation (EC.12) (up to $O(\varepsilon^2)$).

Now turn to the state region in which $t < \max\{t_{0,a}, t_{0,b}\}$. For notational simplicity, we use $X^{buy,\varepsilon}(t,\mu,d_a,d_b)$ and $X^{sell,\varepsilon}(t,\mu,d_a,d_b)$ to denote the parametric forms of the buy and sell boundaries $\widehat{\mathcal{BR}}_t^\varepsilon$ and $\widehat{\mathcal{SR}}_t^\varepsilon$, respectively. Expand the functions F, $X^{buy,\varepsilon}$ and $X^{sell,\varepsilon}$ in terms of ε; that is,

$$F(t,\mu,x,d_a,d_b) = F_0(t,\mu,x,d_a,d_b) + \varepsilon F_1(t,\mu,x,d_a,d_b) + O(\varepsilon^2), \tag{EC.16}$$

$$X^{buy/sell,\varepsilon}(t,\mu,d_a,d_b) = X_0^{buy/sell}(t,\mu,d_a,d_b) + \varepsilon X_1^{buy/sell}(t,\mu,d_a,d_b) + O(\varepsilon^2), \tag{EC.17}$$

ec9

where the functions F_0, F_1, $X_0^{buy/sell}$, $X_1^{buy/sell}$ are to be determined. Substituting (EC.16) and (EC.17) into the system (EC.13) leads to several observations. First, in $\mathcal{NR}$, we have

$$\frac{\partial F}{\partial t} + \mu x - \frac{1}{2}\sigma^2\gamma x^2 + \varepsilon\kappa(\bar{\mu}-\mu)\frac{\partial F}{\partial \mu} + \frac{1}{2}\varepsilon^2\beta^2[\frac{\partial^2 F}{\partial \mu^2} - \gamma(\frac{\partial F}{\partial \mu})^2] - \rho_a d_a \frac{\partial F}{\partial d_a} - \rho_b d_b \frac{\partial F}{\partial d_b}$$

$$= \frac{\partial F_0}{\partial t} + \mu x - \frac{1}{2}\sigma^2\gamma x^2 - \rho_a d_a \frac{\partial F_0}{\partial d_a} - \rho_b d_b \frac{\partial F_0}{\partial d_b} + \varepsilon\Big\{\frac{\partial F_1}{\partial t} + \kappa(\bar{\mu}-\mu)\frac{\partial F_0}{\partial \mu} - \rho_a d_a \frac{\partial F_1}{\partial d_a} - \rho_b d_b \frac{\partial F_1}{\partial d_b}\Big\} + O(\varepsilon^2)$$

$$= 0.$$

Second, the boundaries $X^{buy,\varepsilon}$ and $X^{sell,\varepsilon}$ satisfy

$$\Big(\frac{1}{q_a}\frac{\partial F}{\partial d_a} + \frac{\partial F}{\partial x} - d_a\Big)\big|_{x=X_0^{buy}+\varepsilon X_1^{buy}+O(\varepsilon^2)}$$

$$= \Big(\frac{1}{q_a}\frac{\partial F_0}{\partial d_a} + \frac{\partial F_0}{\partial x} - d_a\Big)\big|_{x=X_0^{buy}} + \varepsilon\Big\{X_1^{buy}(\frac{1}{q_a}\frac{\partial^2 F_0}{\partial x\partial d_a} + \frac{\partial^2 F_0}{\partial x^2}) + \frac{1}{q_a}\frac{\partial F_1}{\partial d_a} + \frac{\partial F_1}{\partial x}\Big\}\big|_{x=X_0^{buy}} + O(\varepsilon^2)$$

$$= 0,$$

and

$$\Big(\frac{1}{q_b}\frac{\partial F}{\partial d_b} - \frac{\partial F}{\partial x} - d_b\Big)\big|_{x=X_0^{sell}+\varepsilon X_1^{sell}+O(\varepsilon^2)}$$

$$= \Big(\frac{1}{q_b}\frac{\partial F_0}{\partial d_b} - \frac{\partial F_0}{\partial x} - d_b\Big)\big|_{x=X_0^{sell}} + \varepsilon\Big\{X_1^{sell}(\frac{1}{q_b}\frac{\partial^2 F_0}{\partial x\partial d_b} - \frac{\partial^2 F_0}{\partial x^2}) + \frac{1}{q_b}\frac{\partial F_1}{\partial d_b} - \frac{\partial F_1}{\partial x}\Big\}\big|_{x=X_0^{sell}} + O(\varepsilon^2)$$

$$= 0.$$

Comparing the coefficients of ε in different orders in the above PDEs, we can derive the following systems of differential equations. Specifically, the equations from the 0-order is

$$\begin{cases} \frac{\partial F_0}{\partial t} + \mu x - \frac{1}{2}\sigma^2\gamma x^2 - \rho_a d_a \frac{\partial F_0}{\partial d_a} - \rho_b d_b \frac{\partial F_0}{\partial d_b} = 0 & \text{in } \mathcal{NR}_0, \\[2mm] \frac{1}{q_a}\frac{\partial F_0}{\partial d_a} + \frac{\partial F_0}{\partial x} - d_a = 0 & \text{on } x = X_0^{buy}, \\[2mm] \frac{1}{q_b}\frac{\partial F_0}{\partial d_b} - \frac{\partial F_0}{\partial x} - d_b = 0 & \text{on } x = X_0^{sell}, \\[2mm] F_0(T,\mu,x,d_a,d_b) = 0. \end{cases} \tag{EC.18}$$

And the equations from the 1st-order comparison are

$$\begin{cases} \frac{\partial F_1}{\partial t} + \kappa(\bar{\mu}-\mu)\frac{\partial F_0}{\partial \mu} - \rho_a d_a \frac{\partial F_1}{\partial d_a} - \rho_b d_b \frac{\partial F_1}{\partial d_b} = 0 & \text{in } \mathcal{NR}_0, \\[2mm] X_1^{buy}(\frac{1}{q_a}\frac{\partial^2 F_0}{\partial x\partial d_a} + \frac{\partial^2 F_0}{\partial x^2}) + \frac{1}{q_a}\frac{\partial F_1}{\partial d_a} + \frac{\partial F_1}{\partial x} = 0 & \text{on } x = X_0^{buy}, \\[2mm] X_1^{sell}(\frac{1}{q_b}\frac{\partial^2 F_0}{\partial x\partial d_b} - \frac{\partial^2 F_0}{\partial x^2}) + \frac{1}{q_b}\frac{\partial F_1}{\partial d_b} - \frac{\partial F_1}{\partial x} = 0 & \text{on } x = X_0^{sell}, \\[2mm] F_1(T,\mu,x,d_a,d_b) = 0. \end{cases} \tag{EC.19}$$

We have already solved F_0 in (EC.18) in Lemma EC.2.1. Substitute F_0 into (EC.19). Note that the equation (EC.19) is a first-order linear PDE. We can use the method of characteristics to solve

ec10

it; refer to, e.g., Section 3.2 of Evans (2002). We omit detailed calculation here in the interest of space. The final solutions are summarized as follows.

Let $a_{01,i}$ and $b_{01,i}$ be the solutions to the following ODE system, $i = a, b$:

$$\begin{cases} (h_i(t) + q_i)a'_{01,i}(t) - \rho_i q_i a_{01,i}(t) + \frac{2\kappa}{\sigma^2\gamma} f_i(t)(h_i(t) + q_i) = 0, \\ b'_{01,i}(t) + \frac{1}{\sigma^2\gamma} a'_{01,i}(t) - \frac{\kappa}{\sigma^2\gamma}(T - t) = 0, \end{cases}$$

where h_i and f_i are defined in (EC.8) and (EC.9), respectively. There are three cases for F_1:

Case (i) If

$$\frac{\mu}{\sigma^2\gamma} - \frac{\rho_a}{\sigma^2\gamma} e^{-\rho_a(T - \frac{1}{\rho_a} - t)} d_a < x < \frac{\mu}{\sigma^2\gamma} + \frac{\rho_b}{\sigma^2\gamma} e^{-\rho_b(T - \frac{1}{\rho_b} - t)} d_b,$$

then,

$$F_1(t, \mu, x, d_a, d_b) = -\frac{1}{2}\kappa(\bar{\mu} - \mu)(T - t)^2 x.$$

Case (ii) If

$$\frac{\mu}{\sigma^2\gamma} - h_a(t)d_a + \varepsilon \frac{a'_{01,a}(t) + \frac{2\kappa}{\sigma^2\gamma} f_a(t)}{2(f'_a(t) - \frac{1}{2}\sigma^2\gamma)}\kappa(\bar{\mu} - \mu) < x < \frac{\mu}{\sigma^2\gamma} - \frac{\rho_a}{\sigma^2\gamma} e^{-\rho_a(T - \frac{1}{\rho_a} - t)} d_a,$$

then

$$F_1(t, \mu, x, d_a, d_b) = \kappa(\bar{\mu} - \mu)\int_0^{\tau - t} \kappa \frac{\partial F_0}{\partial \mu}\left(s + \tau, \mu, x, d_a e^{-\rho_a(\tau - t + s)}, d_b e^{-\rho_b(\tau - t + s)}\right) ds$$
$$- [a_{01,a}(\tau)(x - q_a d_a e^{-\rho_a(\tau - t)}) + b_{01,a}(\tau)\mu]\kappa(\bar{\mu} - \mu),$$

with τ being determined by

$$x - \frac{\mu}{\sigma^2\gamma} + h_a(\tau)e^{-\rho_a(\tau - t)} d_a = 0,$$

Case (iii) If

$$\frac{\mu}{\sigma^2\gamma} + \frac{\rho_b}{\sigma^2\gamma} e^{-\rho_b(T - \frac{1}{\rho_b} - t)} d_b < x < \frac{\mu}{\sigma^2\gamma} + h_b(t)d_b + \varepsilon \frac{a'_{01,b}(t) + \frac{2\kappa}{\sigma^2\gamma} f_b(t)}{2(f'_b(t) - \frac{1}{2}\sigma^2\gamma)}\kappa(\bar{\mu} - \mu),$$

then

$$F_1(t, \mu, x, d_a, d_b) = \kappa(\bar{\mu} - \mu)\int_0^{\tau - t} \kappa \frac{\partial F_0}{\partial \mu}\left(s + \tau, \mu, x, d_a e^{-\rho_a(\tau - t + s)}, d_b e^{-\rho_b(\tau - t + s)}\right) ds$$
$$- [a_{01,b}(\tau)(x + q_b d_b e^{-\rho_a(\tau - t)}) + b_{01,b}(\tau)\mu]\kappa(\bar{\mu} - \mu),$$

with τ being determined by

$$x - \frac{\mu}{\sigma^2\gamma} - h_b(\tau)e^{-\rho_b(\tau - t)} d_b = 0.$$

ec11

So far we have explicitly determined F_0 and F_1 in the expansion (EC.16) to solve the variational inequality (EC.7). From the above (EC.14), (EC.15), cases (ii) and (iii), we also have derived approximations to the buy and sell boundaries. Specifically, define

$$r_i(t) = \begin{cases} \frac{\kappa\sigma^2\gamma}{2} \frac{a'_{01,i}(t) + \frac{2\kappa}{\sigma^2\gamma} f_i(t)}{f'_i(t) - \frac{1}{2}\sigma^2\gamma}, & \text{if } t < T - \frac{1}{\rho_i}, \\[2ex] \frac{\kappa(T-t)}{2}, & \text{if } t \geq T - \frac{1}{\rho_i}, \end{cases} \tag{EC.20}$$

for $i = a, b$. The investor should buy stock whenever the current stock holding position X_t is less than

$$\frac{\mu}{\sigma^2\gamma} - h_a(t)d_a + \varepsilon r_a \frac{\bar{\mu} - \mu}{\sigma^2\gamma}.$$

In other words, the buy region boundary is given by

$$\partial\widehat{\mathcal{BR}_t^\varepsilon} = \left\{ (x, d_a, d_b) \in \mathcal{S} : x - \frac{\hat{\mu}_t^a}{\sigma^2\gamma} = -h_a(t)d_a \right\}.$$

Similarly, we can show the sell region.   Q.E.D.

EC.5.   The Skorokhod Problem and the Gradual Buying/Selling Strategy in the Presence of Signals

The gradual buying and selling part of the trading strategy in the general case keeps the state variables (X_t, D_t^a, D_t^b) staying within the no-trade region once either the buy or sell boundaries is reached. Observe that the movement of both boundaries over time is driven by μ_t, which contains the randomness caused by dW'_t (cf. (23)). Thus, a more accurate description on this part involves the local time of μ_t. To this end, we need to establish the following proposition by invoking the celebrated Skorokhod equation (See Lemma 3.6.14 of Karatzas and Shreve (1991)):

Proposition EC.5.1 *For $i = a, b$, let $z_0^t = X_0 - \hat{\mu}_0^i/(\gamma\sigma^2) + h_i(0)D_0^i$ and denote*

$$z_t^i = z_0^i - \frac{\hat{\mu}_t^i - \hat{\mu}_0^i}{\gamma\sigma^2} + \int_0^t (h'_i(s) - \rho_i h_i(s))D_s^i \mathrm{d}s.$$

Assume that $z_0^a \geq 0$ (resp. $z_0^b \leq 0$). Then, there exist continuous processes $\{k_t^i : t \geq 0\}$, $i = a, b$, such that

(i) $y_t^a := z_t^a + (1 + 1/q_a)k_t^a \geq 0$ (resp. $y_t^b := z_t^b - (1 + 1/q_b)k_t^b \leq 0$), $t > 0$,

(ii) $k_0^i = 0$ and both processes are nondecreasing with respect to t,

(iii) k_t^i is flat off $\{t : y_t^i = 0, t \geq 0\}$; i.e., $1_{\{y_t^a > 0\}}\mathrm{d}k_t^a \equiv 0$ (resp. $1_{\{y_t^b < 0\}}\mathrm{d}k_t^b \equiv 0$) for all t.

Proof. Note that z_t^i is a continuous process for $i = a, b$. This proposition is a direct corollary of the Skorokhod equation.   Q.E.D.

Use the above local-time processes k_t^i, $i = a, b$, we define

ec12

- **Gradual buying and selling**. If (x, d_a, d_b) is on the boundary $\partial \widehat{\mathcal{BR}}_t^{\bar{\varepsilon}}$, $\mathrm{d}L_t^* = dk_t^a$ and $\mathrm{d}M_t^* = 0$. Under this strategy, it is easy to see that

$$
\begin{aligned}
\mathrm{d}\left[X_t - \frac{\hat{\mu}_t^a}{\sigma^2 \gamma} + h_a(t)D_t^a\right] &= \mathrm{d}L_t^* - \frac{\mathrm{d}\hat{\mu}_t^a}{\gamma\sigma^2} + h_a'(t)D_t^a\mathrm{d}t + \left(-\rho h_a(t)D_t^a\mathrm{d}t + \frac{\mathrm{d}L_t^*}{q_a}\right) \\
&= -\frac{\mathrm{d}\hat{\mu}_t^a}{\gamma\sigma^2} + (h_a'(t) - \rho_a h_a(t))D_t^a\mathrm{d}t + (1 + \frac{1}{q_a})\mathrm{d}k_t^a
\end{aligned}
$$

whenever $(X_t, D_t^a, D_t^b) \in \partial \widehat{\mathcal{BR}}_t^{\bar{\varepsilon}}$. The local time $\mathrm{d}k_t^a$ ensures that this gradual buying strategy keeps the portfolio within the no-trade region according to Proposition EC.5.1. Similarly, we can define the gradual selling as follows: if (x, d_a, d_b) is on the boundary $\partial \widehat{\mathcal{SR}}_t^{\bar{\varepsilon}}$, $\mathrm{d}L_t^* = 0$ and $\mathrm{d}M_t^* = -\mathrm{d}k_t^b$.

ec13